

SPECTRA OF TURBULENT FLUCTUATIONS
OVER OCEAN WAVES

Glenn Stevenson Bingham

NAVAL POSTGRADUATE SCHOOL

Monterey, California



THESIS

SPECTRA OF TURBULENT FLUCTUATIONS
OVER
OCEAN WAVES

by

Glenn Stevenson Bingham

Thesis Advisor:

K.L. Davidson

September 1972

Approved for public release; distribution unlimited.

T149511

Spectra of Turbulent Fluctuations
over
Ocean Waves

by

Glenn Stevenson Bingham
Lieutenant Commander, United States Navy
B.A., Emory and Henry College, 1963

Submitted in partial fulfillment of the
requirements for the degree of

MASTER OF SCIENCE IN METEOROLOGY

from the
NAVAL POSTGRADUATE SCHOOL
September 1972

ABSTRACT

Spectral analyses are performed on turbulence data obtained over natural ocean waves during BOMEX. Results are obtained for variance and co-variance spectra, phase and coherence relationships, and amplitude ratios. Peaks in the horizontal and vertical velocity spectra are observed to correspond to the frequency of the wave spectra peaks. Phase relationships tend to obey predictions of potential flow theory in regions of the wave spectra peaks. However, the wave related motion contributes to the momentum transfer which is not predicted by potential flow theory. The ratio of the wave induced disturbance to the sea surface displacement is used to locate the wave spectra frequency for which the level of measurement is a critical level. Results of the study are readily compared to existing wind-wave coupling theories, both linear and non-linear.

TABLE OF CONTENTS

I.	INTRODUCTION -----	7
II.	BACKGROUND -----	9
	2.1 THEORETICAL BACKGROUND -----	9
	2.2 OBSERVATIONAL BACKGROUND -----	11
	2.2.1 Results of Kondo et al. -----	12
	2.2.2 Results of Davidson -----	15
III.	MEASUREMENTS AND ANALYSES -----	19
	3.1 MEASUREMENTS -----	19
	3.2 ANALYSES -----	20
	3.2.1 Initial Data Preparation -----	22
	3.2.2 Data Reduction and Analyses -----	23
IV.	PRESENTATION OF RESULTS -----	28
	4.1 VARIANCE SPECTRA -----	30
	4.2 CO-VARIANCE SPECTRA -----	38
	4.3 PHASE-COHERENCE RELATIONSHIPS -----	39
	4.4 AMPLITUDE RATIO RESULTS -----	48
	4.5 RESULTS AT THE 3 METER LEVEL -----	53
V.	CONCLUSIONS -----	57
	BIBLIOGRAPHY -----	59
	INITIAL DISTRIBUTION LIST -----	61
	FORM DD 1473 -----	63

LIST OF FIGURES

1.	Model of Miles' wind-wave coupling theory showing consequences of dynamics at critical level -----	10
2.	Samples of Spectral Results including power density spectra, phase, coherence, and amplitude ratio, from Kondo et al. (1972) -----	13
3.	Sample of Variance and Co-variance Spectral Results, from Davidson and <u>Franks</u> (1973) -----	16
4.	Sample of Phase and Coherence Spectra, from Davidson (1970) -----	18
5.	Sensor locations on FLIP -----	20
6.	Initial data processing flow diagram -----	21
7.	Period 1. Variance, Co-Variance Spectral Results ---	31
8.	Period 2. Variance, Co-Variance Spectral Results ---	32
9.	Period 3. Variance, Co-Variance Spectral Results ---	33
10.	Period 4. Variance, Co-Variance Spectral Results ---	34
11.	Period 5. Variance, Co-Variance Spectral Results ---	35
12.	Period 6. Variance, Co-Variance Spectral Results ---	36
13.	Period 1. Phase and Coherence Spectral Results -----	40
14.	Period 2. Phase and Coherence Spectral Results -----	41
15.	Period 3. Phase and Coherence Spectral Results -----	42
16.	Period 4. Phase and Coherence Spectral Results -----	43
17.	Period 5. Phase and Coherence Spectral Results -----	44
18.	Period 6. Phase and Coherence Spectral Results -----	45
19.	Periods 1 and 2. Amplitude Ratio Results -----	49
20.	Periods 3 and 4. Amplitude Ratio Results -----	50
21.	Periods 5 and 6. Amplitude Ratio Results -----	51
22.	Period 7. Variance and Co-Variance Spectral Results -----	54

23.	Period 7.	Phase and Coherence Spectral Results ---	55
24.	Period 7.	Amplitude Ratio Results -----	56

ACKNOWLEDGEMENTS

The successful completion of this research project would not have been possible without the guidance and encouragement of many persons. The author is especially indebted to his advisor and friend, Professor Kenneth L. Davidson, who spent many hours advising, assisting, and supporting him in his work. Appreciation is also expressed to Professor Edward B. Thornton for his thorough review of the manuscript and helpful suggestions, and to Miss Sharon Raney, Staff Programmer, for her guidance in computer programming. Also, gratitude is expressed to Mrs. Rosemary Lande who typed the final manuscript.

The Office of Naval Research made this research possible through contract N 00014-67-A-0181-0005 with the University of Michigan and Task NR083-265 with the U.S. Naval Post-graduate School.

Most importantly, a most sincere and grateful "Thank You" to my lovely wife, Priscilla, for her infinite patience, understanding, and love throughout this venture. Thanks, again, to Priscilla for the many late night hours spent typing the several versions of the rough manuscript. And, finally, to my children, Glenn, Trina, and David, an apology for the many nights away from home, and a deep appreciation for your unselfishness.

I. INTRODUCTION

Several applied problems, especially long range atmospheric prediction, have created considerable interest recently in the contributory effects of the near surface boundary layer over the oceans. For example, Zilitinkevich (1969) has stated that long range atmospheric prediction models will require proper description of the effects of sea-air interaction. Such descriptions will, most likely, include estimates of energy exchange in the near surface layer. Furthermore, calculating these estimates requires a comprehension of the mechanisms governing sea-air interaction processes.

An important sea-air interaction concept is that of the wind-wave coupling. Recent theories of wind-wave coupling have been proposed by Miles (1957) and Yefimov (1970). Unfortunately, theoretical aspects of wind-wave coupling have progressed much more rapidly than actual observational studies. However, significant progress occurred in 1969 with respect to observational studies as a result of the "Barbados Oceanographic and Meteorological Experiment" (BOMEX).

BOMEX took place in the Atlantic Ocean east-northeast of Barbados, West Indies. The area of interest was contained in a volume 500 km square and from 500 m below the sea surface to three miles above it. The experiment was perhaps one of the largest environmental research programs ever

undertaken. It consisted of over 80 subprograms. One of these subprograms, titled "sea-air interaction," is significant to this study because it dealt with the measurement of heat and momentum exchange between the sea and the near surface layer of the atmosphere.

Various oceanic platforms were used in the collection of near-surface data but one was of particular interest. That was the "Floating Instrument Platform" (FLIP).¹ The data to be considered in this report was collected from FLIP.

The primary purpose of this study is to perform spectral analyses on the velocity data obtained near the surface and compare the results with those predicted by existing wind-wave coupling theories. A secondary purpose is to attempt simultaneous investigations of the linear and non-linear interactions occurring between the ocean waves and airflow in the near surface boundary layer.

¹FLIP was developed by the Marine Physical Laboratory of The University of California, San Diego and Scripps Institute of Oceanography. For more information on FLIP see Bronson and Glasten (1965).

II. BACKGROUND

It has long been accepted that a wind blowing across water will cause waves. However, very few theories on how the wind caused waves have been advanced until recently. In an early study, Jefferys (1924) discussed the minimum wind necessary to cause waves using the effects of normal stresses. Later, Phillips (1957) provided a significant theory on how a turbulent wind advecting over an initially still body of water causes waves. This "wave generation" theory of Phillips was soon complemented with a wind-wave coupling theory by Miles (1957). Recently, spectral analyses on over water velocity data have provided observational results which can be used to evaluate features inherent in Miles' theory.

2.1 THEORETICAL BACKGROUND

In this section aspects of wind-wave coupling theories will be reviewed briefly. First to be considered are aspects of Miles' theory. The primary features of the air-flow in this theory are depicted in Figure 1. An essential concept in Miles' theory is the existence of the critical level, the level where the wind speed is equal to the phase speed of the perturbing wave. The critical level (Z_c) is denoted by a dashed line in Figure 1 in a coordinate system which is stationary with respect to the wave phase speed. Below Z_c the airflow appears to be moving in a negative

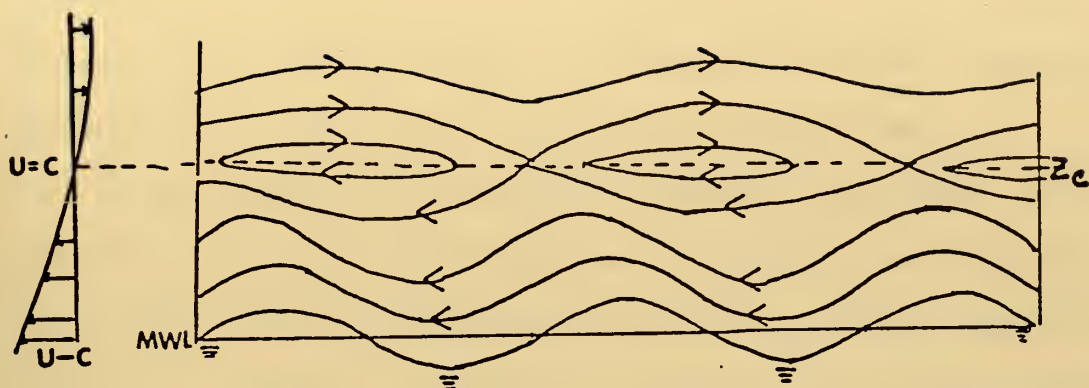


Figure 1. Model of Miles' Wind-Wave Coupling theory showing consequences of dynamics at critical level, from Davidson (1970).

direction since the wind speed is less than the phase speed of the wave. Above Z_c the wind speed exceeds the wave speed, and hence the flow appears to move in a direction opposite that below.

A definite sinusoidal phase relationship between the wind and waves is depicted in Figure 1 above and below Z_c , while at Z_c no such relationship appears. The latter leads to the fact that no phase relationship can be defined at this level since the mean wind is moving at the same speed as the disturbing wave. Through this level, though, a phase shift occurs between the fluctuations in the airflow and the water surface elevation. Lighthill (1962) has related the shift to the dynamics of the critical level which involves the transfer of vorticity through Z_c . A lesser amount of vorticity is transported downward than upward across Z_c .

The result is a net vortex acceleration at the critical level. This negative mean acceleration extracts momentum from the mean wind and transfers it to the wave.

Miles' theoretical model is essentially linear in nature since, in the model, turbulence in the airflow is neglected except for its role in maintaining the mean wind profile. Recently, however, a wind-wave coupling theory was advanced by Yefimov (1970) wherein the effects of turbulence in the airflow were considered. In Yefimov's model dynamics at the critical level are not the only reason for wave related motion to deviate from potential flow predictions.

Potential flow predictions apply to the fluctuations observed at a fixed level in a shear flow above a progressive wave. The horizontal wind component differs from the wave by 180 degrees, and the vertical wind component leads the wave by 90 degrees. Because u and w are 90 degrees out of phase in such a case, the u momentum transfer, uw , would be zero. Yefimov, however, obtained numerical results which indicate that momentum transfer, uw , is not zero due to the non-linear interaction between the wave induced motion and the turbulence in the airflow.

2.2 OBSERVATIONAL BACKGROUND

The theoretical investigations of wind wave-wave coupling appear to have progressed at a steady rate but, as Stewart (1967) has noted, the availability of overwater measurements has been insufficient to either verify or

modify existing theories. The situation, however, has improved considerably over the last five years. Recent observational studies have been described by Pond, et al. (1971), Yefimov and Sizov (1969), Davidson (1970), Kondo, et al. (1972), and several others. Two investigations of particular importance to this thesis are those by Kondo, et al. and Davidson. These reports will be discussed in detail below.

2.2.1 Results of Kondo et al.

Kondo et al. performed spectral analyses on data obtained from a marine tower in Sagami Bay, Japan. The results were compared with the predictions of inviscid theory. Their study was limited to the relationships of the horizontal wind fluctuation to the sea surface displacement, thus omitting any consideration of the vertical fluctuations. This is unfortunate since the vertical velocity fluctuation is important in the existing theories and also in any examination of momentum transfer processes. The vertical velocity component was available for consideration in the present study.

The results of Kondo et al. revealed a peak in the velocity spectra at the frequency of the wave spectrum peak (Figure 2a). Also, a maximum value of coherence (Figure 2c) was centered around this frequency. The latter result is indicative of the high correlation between the horizontal wind fluctuations and the sea surface displacement. With respect to phase relationships between the

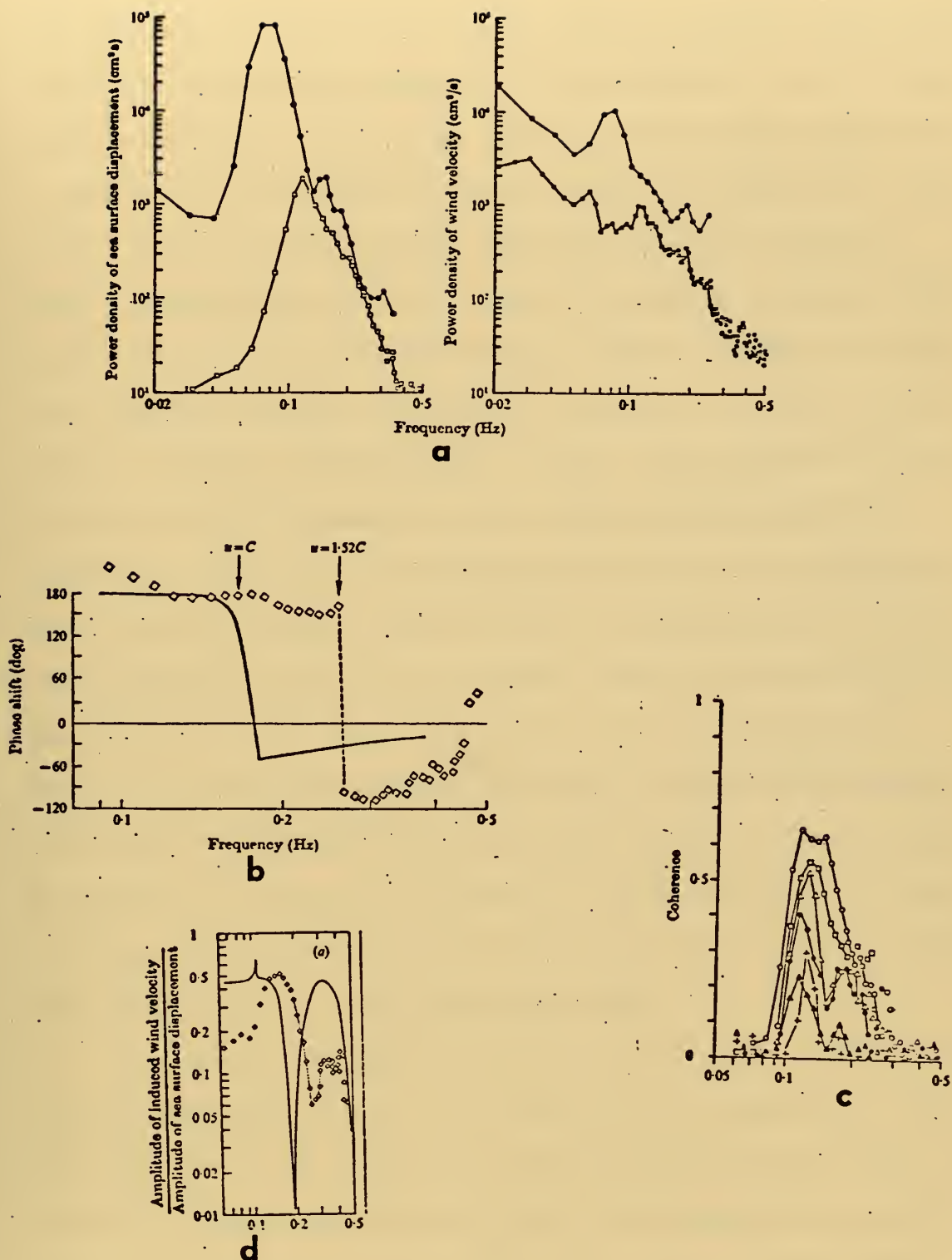


Figure 2. Samples of: (a) sea surface displacement and velocity power spectra, (b) phase shift between u and waves, (c) coherence values, and (d) amplitude ratio, from Kondo et al. (1972).

fluctuating horizontal wind and the sea surface displacement, the phase difference appeared to be dependent on the relative velocities of the mean wind and the propagating wave. A sample of their phase results appears in Figure 2b. In this figure the heavy solid line denotes the inviscid theory prediction and the series of squares represent the mean of two sets of observations. The u component of the fluctuating wind was, therefore, observed to differ from the sea surface displacement by about 180 degrees in the 0.1 to 0.25 Hz frequency range, then becoming negative abruptly. The abrupt frequency reversal is in agreement with inviscid theory except that the actual phase reversal was observed to occur at a higher frequency than predicted. Specifically, the phase reversal occurred at the wave frequency whose phase speed was equal to about two-thirds the speed of the mean airflow at the level of measurement. In general, Kondo et al. found the phase reversal to occur at the point where the mean wind speed was 1.2 to 1.5 times the phase speed of the perturbing wave.

They also examined a spectral statistic referred to as the amplitude ratio (to be described in section 3.2.2). This statistic was useful in the discerning of the frequency of phase reversal even when the background turbulence was large relative to the wave induced turbulence. A sample of the amplitude ratio appears in Figure 2d. The solid line denotes the prediction by inviscid theory. The

ratio can be seen to have a minimum at the same frequency (0.25 Hz) where the phase relationship reversed (Figure 2b) and the coherence value dropped to zero.

The work of Kondo et al, was a fortuitous reference for this thesis. Their interpretations with respect to inviscid theory form the primary background against which the results of this present study will be compared.

2.2.2 Results of Davidson

Davidson (1970) examined observational data gathered over waves on Lake Michigan. The data were from simultaneous measurements of wave heights and velocity fluctuations, u and w , at two different levels. He obtained spectral results which were compared to the wind-wave coupling predictions of Miles' theory. In a later paper, Davidson and Franks (1973) considered the role of turbulence in these same data.

Characteristic peaks in the velocity spectra at the frequency of the wave spectra peaks were observed in the Lake Michigan results (Figure 3). Furthermore, momentum transfer from the waves to the airflow at the frequency of the wave spectrum peak was found to occur when the mean wind speed was much less than the phase speed of the dominant wave component. Interpretations of Davidson's results with respect to the proximity of the critical level revealed that the phase relationships between the velocity components and waves were in agreement with the predictions

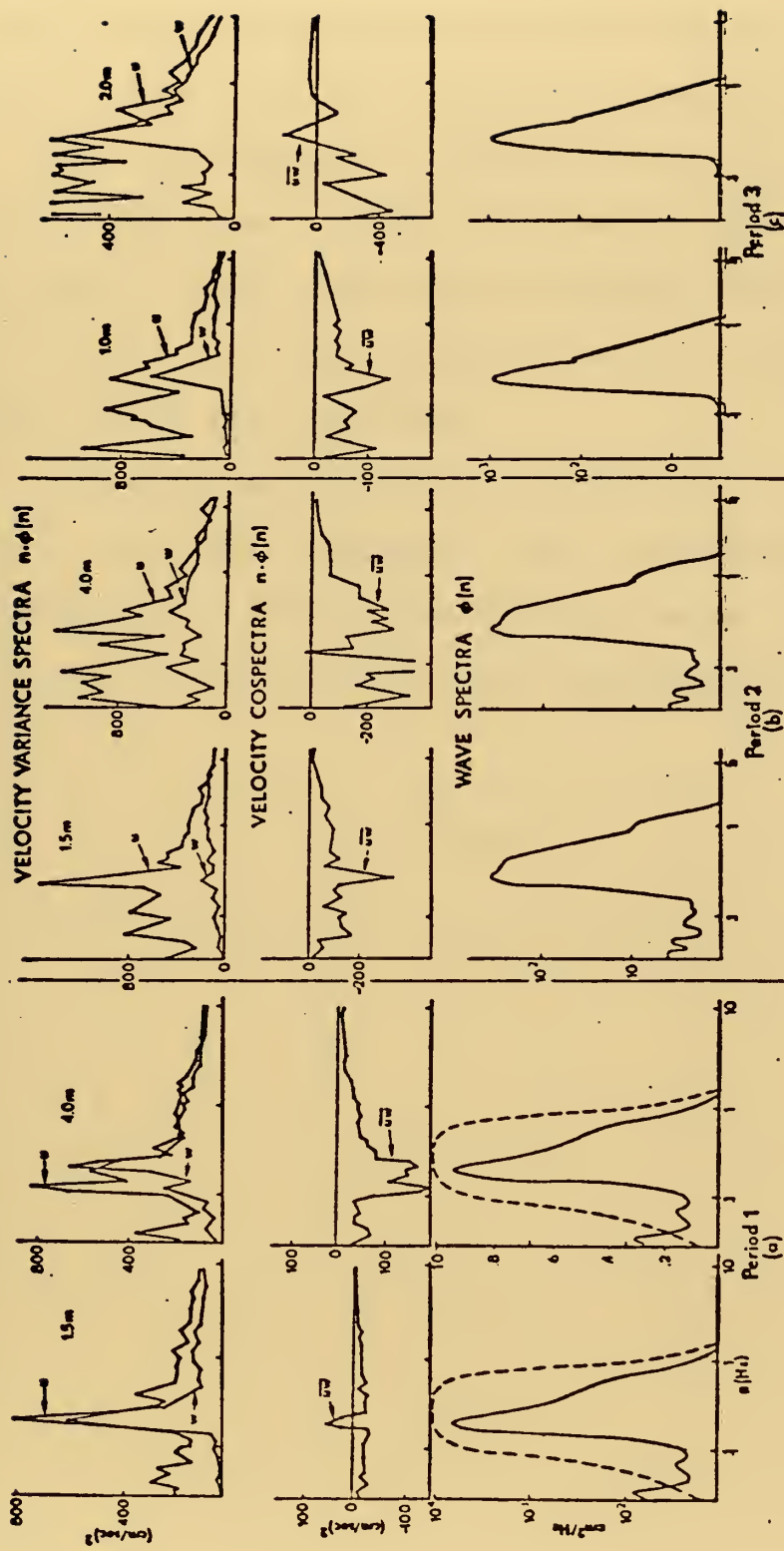


Figure 3. Sample of variance and co-variance results, from Davidson and Franks (1973).

of analytical theory as described by Lighthill (1962).

A sample of Davidson's phase-coherence results appears in Figure 4. His results are similar to those of Kondo et al.

The investigation of Davidson was one of the first and one of the more complete spectral studies of observational data. Also his tested procedures were, in large part, a basis from which spectral analyses procedures used in this thesis were developed.

The results of Davidson, Kondo et al., and the current study which represent three independent experiments should provide a strong observational basis for proper evaluation of existing wind-wave coupling models.

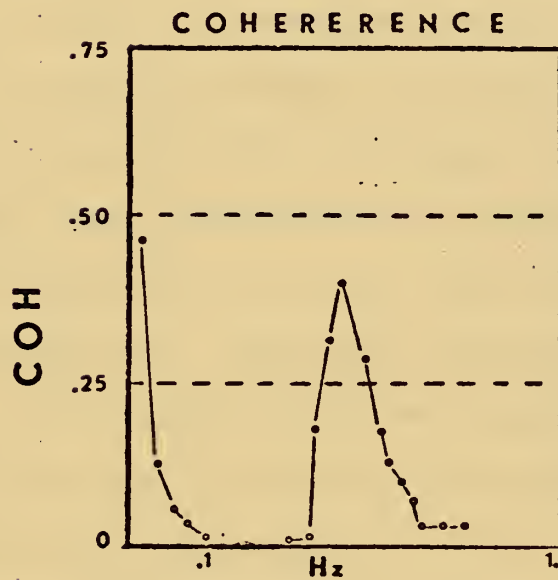
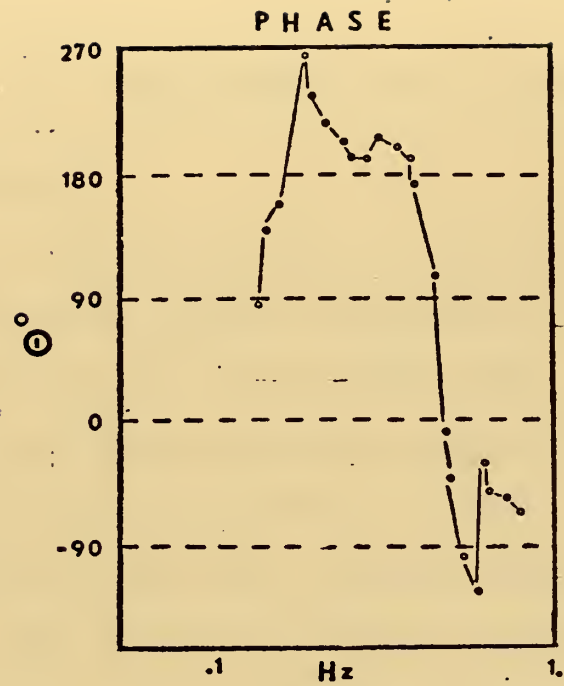


Figure 4. Samples of phase and coherence spectra, from Davidson (1970).

III. MEASUREMENTS AND ANALYSES

3.1 MEASUREMENTS

University of Michigan personnel obtained over 54 hours of measurements in 40 separate observational periods aboard FLIP during the last two weeks of May 1969. Measurements of the three fluctuating velocity components (u , v , and w) were made at the 2, 3, 6 and 8 meter levels (see Figure 5). They were made with hot film, constant temperature anemometer systems. The anemometer systems incorporated linearizers to compensate for the non-linear voltage-velocity relationship. In such a system, the velocity is measured on the basis of heat loss from the heated sensor to the moving air. An advantage of this system is the frequency response, which was over 50 hz (Portman, et al., 1970).

Wave heights were measured with a resistance wave gauge, made available by Dr. R. E. Davis, Scripps Institution of Oceanography. The probe consisted of a nonconducting tube, with a conducting wire wrapped spirally around it. It was positioned about five meters inboard of FLIP's vertical mast (Figure 5).

Sensor outputs were recorded by frequency modulation on two seven channel, magnetic tape recorders using one-quarter inch magnetic tape.¹

¹For details on sensors and recording equipment see Portman, et al., 1970.

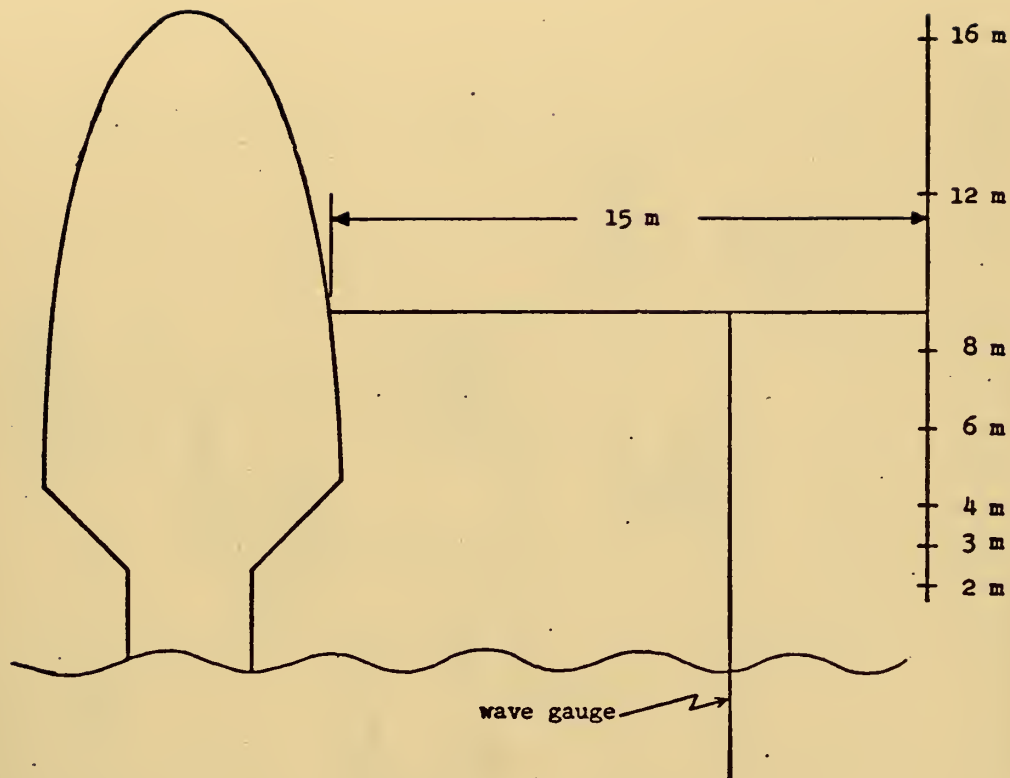


Figure 5. Sensor locations on FLIP, from Portman et al. (1970).

3.2 ANALYSES

The primary objective of the analyses is to describe wind and wave fluctuations on the basis of spectral results. However, before spectral analyses could be applied to the data, several preliminary steps were completed. These initial procedures appear in the flow diagram in Figure 6.

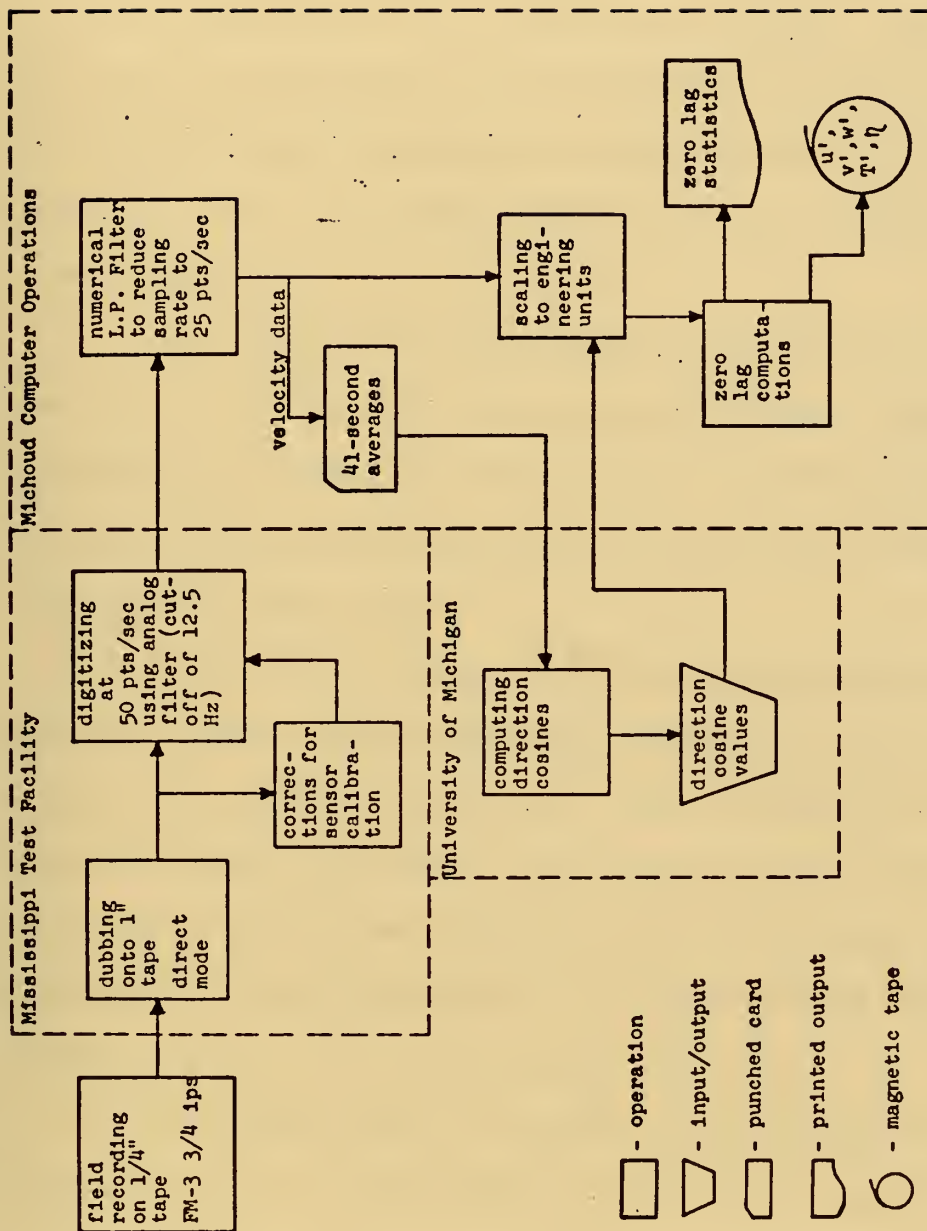


Figure 6. Initial Data Processing, from Portman et al. (1970).

3.2.1 Initial Data Preparation²

Initially, at the NASA Mississippi test facility, Bay St. Louis, the data in analog form had to be reproduced from one-quarter inch magnetic tape onto one inch tape. The data was then digitized at 50 points per second. An analog filter was used to eliminate all frequencies greater than 12.5 hz. At the same time corrections were made to the data for gain and drift errors during recording using available calibration signals.

The digitized records were reduced to 25 points per second at NASA Michoud Computer Operations, Slidell, Louisiana, by numerical filtering. For this, a 5-weight inverse transform filter was used which has a high frequency cut off of about 7 hz.

Direction cosines, which were required for determining the individual wind velocity components (u,v,w), were computed from the hot film data. This procedure was necessary because of the arbitrary orientation of the hot-film anemometer probe during measurements. The direction cosines were computed at the University of Michigan using 41 second averages of the hot-film anemometer data.

The final steps in initial data preparation were to scale the data to engineering units (e.g. cm/sec., degrees centigrade, etc.) and then to compute zero lag statistics (e.g. first, second, third and fourth moments).

²All procedures utilized in the initial data preparation were developed by the Department of Meteorology and Oceanography, University of Michigan, under the direction of Professor D.J. Portman.

3.2.2 Data Reduction and Analyses³

Seven of the forty observational periods were chosen for spectral analyses in this study. However, prior to performing the spectral analyses, four additional procedures were necessary.

First, the over abundance of data (about 120,000 data points per period) had to be reduced to a manageable figure (about 24,000 points per period). This was accomplished using an 11 weight low-pass numerical filter. The sampling rate was reduced from 25 to 5 data points per second.

Second, the removal of the means and trends was necessary so that the time series could be considered statistically stationary. A time series can not be considered stationary if scales of variation exist which are long relative to the record length. The means and trends were removed by forming a best fit in a "least squares" sense to the original time series.

Elimination of erroneous data points was a third necessary procedure. "Dropouts" and "spikes" occasionally appeared in the records due to inherent imperfections in both the magnetic tape and electronic components during the initial recording aboard FLIP. To remove these bad data points each time series was "edited" by comparing the deviation of each data point from the mean with the standard

³All computations in this section were done on the IBM-360 computer in the W.R. Church Computer Facility at the U.S. Naval Postgraduate School, Monterey, California.

deviation. If the deviation exceeded four times the standard deviation the point was replaced with an interpolated value. If a discarded point was the first or last point in a record it was replaced with the mean value.

A final step was to apply a data window to each time series. This diminished the energy drainage between neighboring harmonics. The data window selected for use was the "cosine bell" which Davidson (1970) used and corresponds to the Tukey Spectral Window (Blackman and Tukey, 1958, page 98).

Completion of the four previous procedures resulted in a quasi-stationary time series ready to be transformed into frequency space. The transformation was accomplished using a version of the Fast Fourier Transform, RHARM, (Cooley and Tukey, 1965) which is included in the IBM scientific subroutine package. The transform in this subroutine was the following:

$$x_j = \frac{A_0}{2} + \sum_{n=1}^{N-1} [A_n \cos \left(\frac{j\pi n}{N} \right) + B_n \sin \left(\frac{j\pi n}{N} \right)] \quad (1)$$

where $j = 0, 1, 2, \dots, (2N-1)$

$N = 8192$

$n =$ harmonic number

$x_j =$ variable at time step j

$A_n, B_n =$ Fourier coefficients

8192 pairs of Fourier coefficients were obtained from the transformation of the 16,384 data points. These coefficients were treated in complex form such as $u_n = A_n + iB_n$ (n refers to the nth harmonic) and were used to compute the various spectral estimates.

The variance spectral estimates for each variable were determined for the product of $u(n)$ and its conjugate

$$\phi_{uu}(n) = \frac{T}{2} [A_n + iB_n] \cdot [A_n - iB_n] = \frac{T}{2} [A_n^2 + B_n^2] \quad (2)$$

where T = length of period.

The cross spectral estimates were determined from the product of one complex coefficient ($u(n)$) with the conjugate of another, ($v(n)$),

$$\begin{aligned} \phi_{uv}(n) &= \frac{T}{2} [A_n + iB_n] \cdot [C_n - iD_n] \\ &= \frac{T}{2} [A_n C_n + B_n D_n] + i \frac{T}{2} [B_n C_n - A_n D_n] \end{aligned} \quad (3)$$

The real and imaginary parts of equation 3 are the co-spectral and quadrature spectral estimates respectively:

$$\text{co-spectral; } \phi_{uv}(n) = \frac{T}{2} [A_n C_n + B_n D_n] \quad (4)$$

$$\begin{array}{l} \text{quadrature} \\ \text{spectral; } \phi_{uv}^*(n) = \frac{T}{2} [B_n C_n - A_n D_n] \end{array} \quad (5)$$

The 8192 estimates for variance and cross-variance spectra were reduced to 128 data points by averaging over neighboring harmonics. This was done to improve diagnostic values, and hence eliminate the scatter in the original values, but still retain significant features. The procedure used was similar to one used by Oort and Taylor (1969) and Davidson (1970) and involved averaging over exponentially increasing intervals as the frequency increased. This method results in the final estimates being equally spaced over a logarithmic scale.

The phase relationship ($\bar{\theta}_{un}(n)$) between wind components (u,v,w) and the waves (n) was determined using the co- and quadrature spectral estimates (Equations 4 and 5) as follows:

$$\bar{\theta}_{un}(n) = \arctan [\bar{\phi}_{un}^*(n)/\bar{\phi}_{un}(n)] \quad (6)$$

An estimate of the correlation or association, between the fluctuating wind components and the sea-surface displacement, as a function of frequency is expressed by the coherence. The coherence is the normalized cross-spectral estimate and was also computed from average spectral estimates in the form:

$$\overline{coh}_{un}(n) = [\bar{\phi}_{un}^2(n) + \bar{\phi}_{un}^{*2}(n)]/[\bar{\phi}_{uu}(n) \cdot \bar{\phi}_{nn}(n)] \quad (7)$$

A final statistic computed from average spectral estimates is the ratio of the wave-induced disturbances to

the sea surface displacement, as a function of frequency. This ratio is called, appropriately, the "amplitude ratio" and is used to locate the frequency of the wave component whose phase speed causes the level of measurement to become a "critical level". The amplitude ratio is expressed as

$$(\text{Amplitude Ratio})^2 = [\overline{\phi}_{un}^2(n) + \overline{\phi}_{un}^{*2}(n)] / \overline{\phi}_{nn}^2(n) \quad (8)$$

After all spectral results are obtained they are plotted on a linear-log scale. The variance and co-variance spectral estimates were plotted on the y-axis as a product of the frequency and spectral estimate, $n \cdot \overline{\phi}_{un}(n)$. The x-axis in all plots was plotted as the common logarithm of the frequency. For the phase relationships, the y-axis was scaled from 0 to 360 degrees. The common logarithm of the amplitude ratio, rescaled from 0 to 1, is displayed on the y-axis in those plots.

IV. PRESENTATION OF RESULTS

Spectral results for seven of the 40 observational periods will be presented in this section. A brief meteorological summary of these periods appears in Table 1. The mean wind velocity is shown to be about 10 mps at the eight meter level in all periods except 5 and 6, where it is about 7 mps. The wave heights were visually estimated to be 6-8 feet in 5 of the seven periods. In periods 3 and 4, the wave heights were estimated to be 3-4 feet. During periods 5, 6, and 7, the wave heights were increasing.

The mean directions of the wind and waves were nearly coincident during the seven periods. The relative angle between wind and waves was 5 degrees or less for all periods except for 7 where it was 20 degrees (from Superior, 1969).

The critical level corresponding to the wave spectra peak was well above 10 meters since the phase speed corresponding to this frequency (0.1 hz) was about 15.6 mps for a deep water wave. Thermal stratification of the air for all periods was stable.

The results will be presented individually for variance spectra, co-variance spectra, phase and coherence spectra, and amplitude-ratio spectra. Within each presentation, u, v, and w contributions will be considered separately. Additionally, periods 1-6 will be considered collectively for the 8 meter level. Period 7 at the 3 meter level, will

TABLE 1
METEOROLOGICAL SUMMARY OF ANALYZED PERIODS

Period Designation	Period Number	Date (1969)	Time (GMT)	Period Length (min)	Height Analyzed (m)	Wind Speed (mps)	Wave Heights (ft)	Critical Level (m)
1	A-10	19 May	0308-0429	81	6	10.4	6-8	> 10
2	A-15	19 May	1613-1735	82	8	9.8	6-8	> 10
3	A-24	26 May	2132-2252	83	8	10.1	4	> 10
4	A-25	27 May	0311-0435	84	8	8.8	3	> 10
5	A-39	28 May	1754-1916	82	8	7.6	6-8	> 10
6	A-40	28 May	2028-2150	82	8	6.4	6-8	> 10
7	B-30	27 May	1616-1738	82	3	10.0	7-11	> 10

be considered separately in section 4.3 due to the different features observed closer to the surface.

Variance and co-variance spectral results will be presented in terms of their respective relationships to the wave spectra peak. Results of phase, coherence, and amplitude ratio computations will be compared with the predictions of potential flow theory.

4.1 VARIANCE SPECTRA

Wave spectra for periods 1-6 appear in panel F of Figures 7-12 inclusive. A peak in the wave spectra is observed at a frequency of about 0.1 hz in each period. In panel A of Figure 7 a corresponding peak in the u spectra is seen at the frequency of the wave spectrum peak. The front face of the peak in the u spectra appears to coincide almost exactly with the front face of the wave spectrum peak.

With respect to relative magnitudes of the u spectral peaks, periods 1 and 3 have higher mean wind speeds (Table 1) and thus would be expected to have more background turbulence. The higher background turbulence is revealed by the overall larger values across the spectrum. That this background turbulence tends to mask wave induced perturbations in the airflow is evidenced by the less pronounced peak in u at the wave spectrum peak frequency. Conversely, significant peaks in the u spectra are seen in periods 2, 4, 5, and 6. These peaks, in u, closely approximate the shape

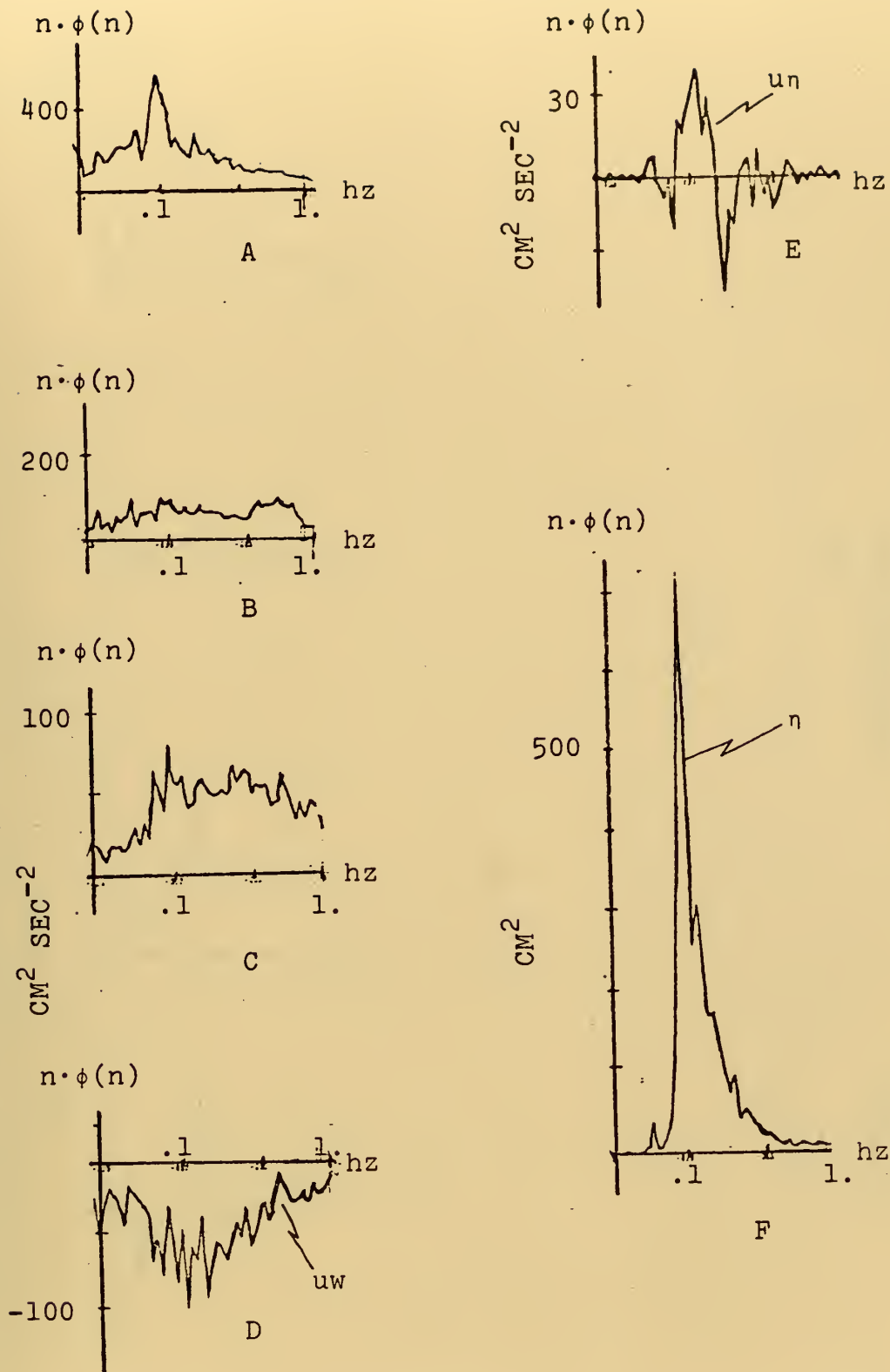


Figure 7. Period 1. Variance and Covariance Spectral Results

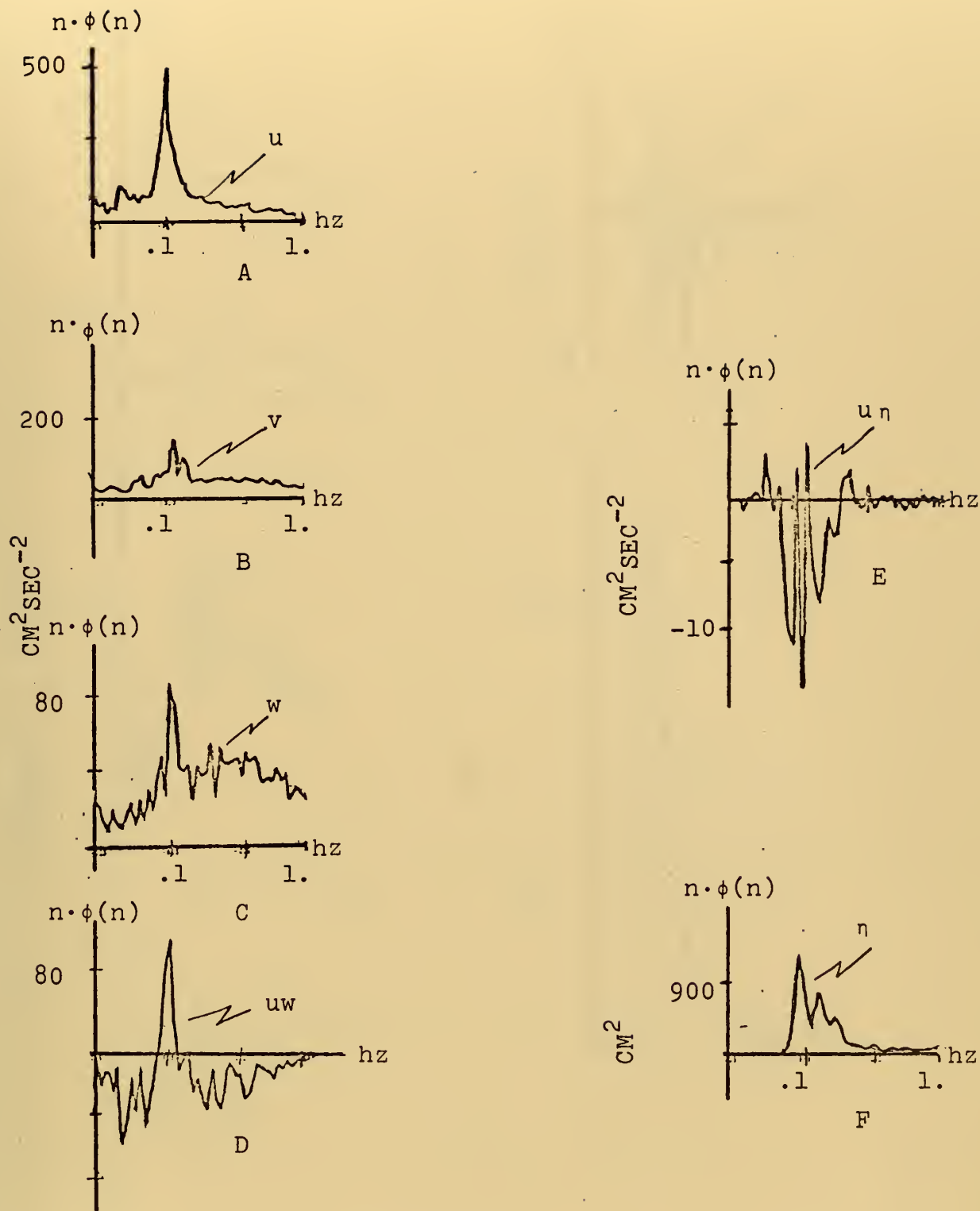


Figure 8. Period 2. Variance and Covariance Spectral Results.

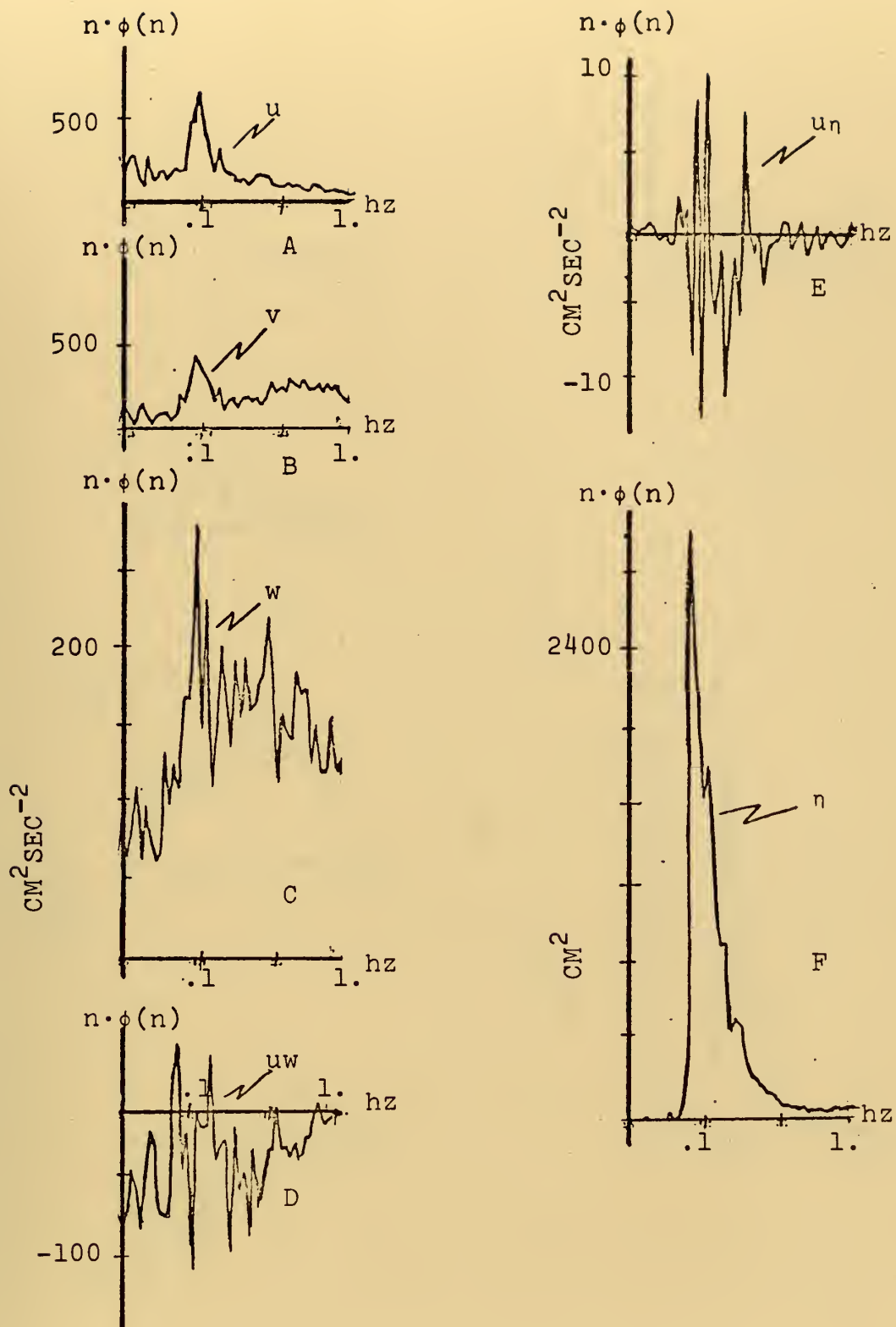


Figure 9. Period 3. Variance and Covariance Spectral Results

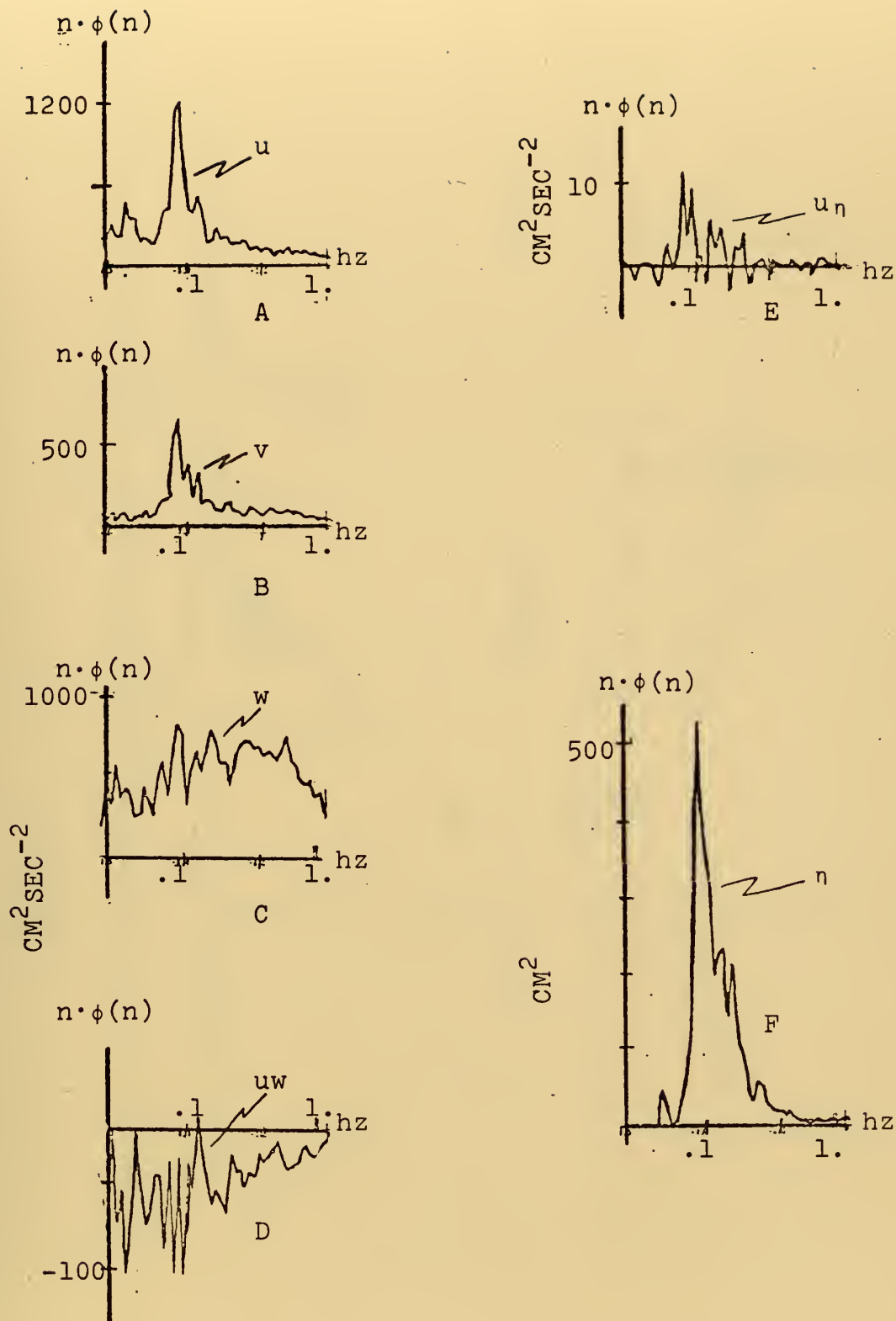


Figure 10. Period 4. Variance and Covariance Spectral Results

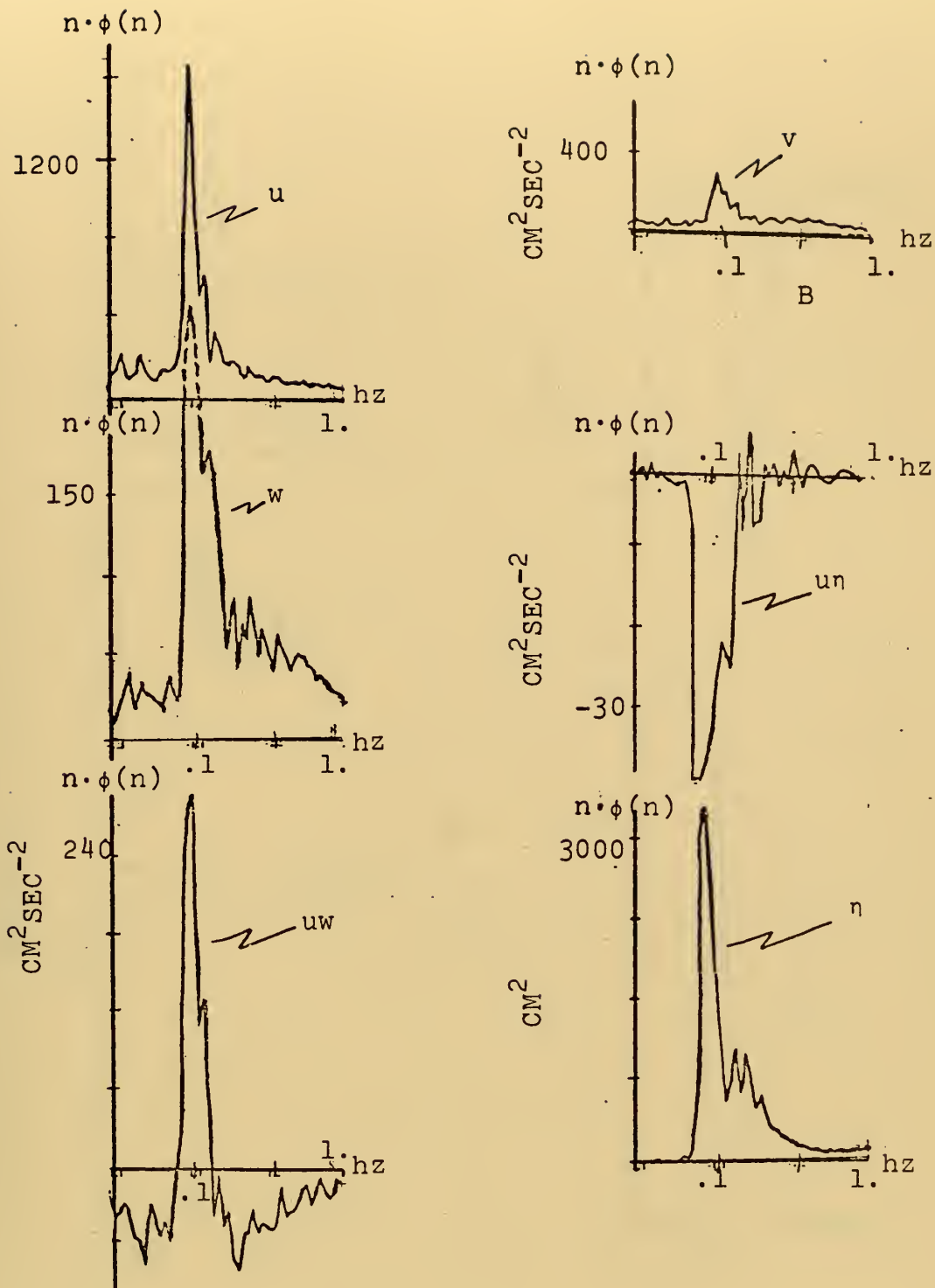


Figure 11. Period 5. Variance and Covariance Spectral Results

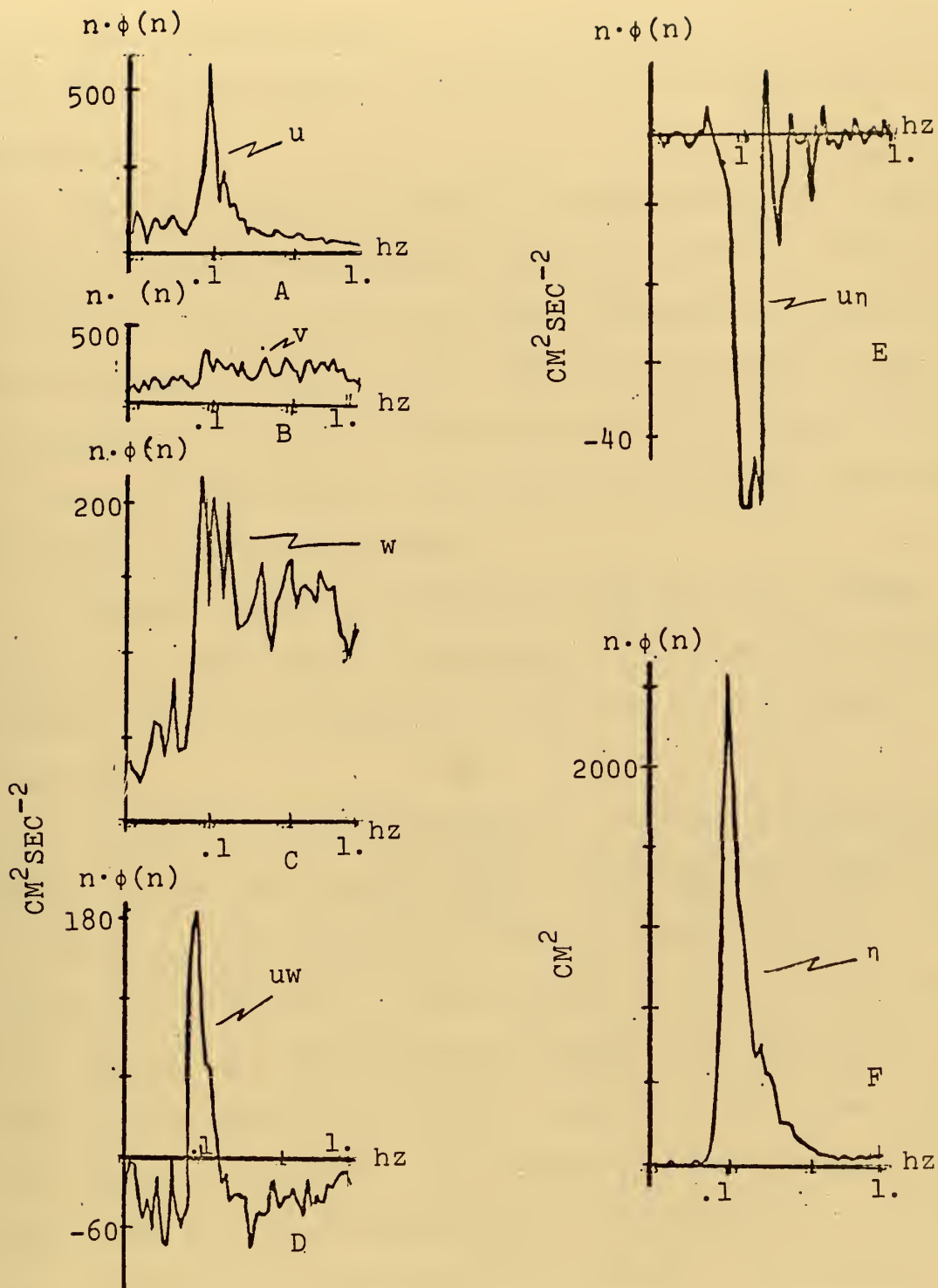


Figure 12. Period 6. Variance and Covariance Spectral Results

of the wave spectra peaks. In these 4 periods, the wind had been decreasing rapidly, resulting in less background turbulence.

V spectra appear in panel B of each figure. No peaks in the v spectra are visible in periods 1 and 6, but for periods 2-5 peaks do exist near the frequency of the wave spectra peaks. Peaks in the v spectra, periods 2-5, are interpreted to be due to the relatively large wave induced lateral wind fluctuation occurring when mean wind and wave propagation directions differ.

W spectra appear in panel C of Figures 7-12. Peaks in the w spectra can be identified for all periods and are centered near the frequency of the wave spectra peaks (0.1 hz).

In period 1, the wave related w spectrum peak does not appear to be significant. This is possible due again to a relatively high magnitude of background turbulence. The background turbulence is also evidenced in the u spectrum for this period. The w peak in period 2 is quite pronounced even though the overall magnitude of the wave spectrum peak is decreased. The prominent w peak is possibly associated with the decreasing mean wind speed and subsequent reduction in background turbulence. The overall w spectrum in period 3 is of relatively high magnitude. This is possibly due to the rapid increase in the mean wind speed which had occurred over the last few hours. Also, as the mean wind speed increased the influence of the waves

on the vertical airflow at this level appeared to diminish. This could be due to the increased winds causing the level of measurement to approach being a critical level with respect to the peak wave spectrum frequency. Recall, that decreased wave influence was evident in the u spectra. In periods 5-6 the mean wind speed had decreased significantly and the peak waves increased influence on the near surface layer airflow was obvious.

4.2 CO-VARIANCE RESULTS

The uw and $u\eta$ cospectra appear in panels D and E, Figures 7-12, respectively. Again, extrema in the cospectra results appear at the frequency of the wave spectra peaks. At the frequency of the wave peaks for periods 2, 5, and 6, an upward u momentum transfer occurs. The distinct, positive uw spectra peaks at this frequency are indicative of the non-linear wind-wave interaction in the near surface layer. This result contrasts with potential flow theory which predicts the overall contribution of uw to be zero since u and w are in quadrature. On the other hand, in periods 1 and 4, a downward momentum transfer is revealed in the presence of higher wind speeds and wave heights. This negative extrema in uw implies that the airflow is, in fact, transferring energy to the waves via a mechanism such as that described by Miles. However, in periods 3 where the mean wind speed was relatively large with small wave heights, the background turbulence seemed to dominate

the uw co-spectrum. In fact, enhanced downward momentum transfer for the period appears only as a very narrow spike at the frequency of the wave spectrum peak.

$U\eta$ cospectra in periods 2, 5, and 6 are observed to obey the predictions of potential flow. It can be recalled that potential flow theory predicts a 180 degree phase shift between u and η . This implies a negative correlation between wind and waves such that over the wave crest the horizontal wind decreases and conversely, over the wave trough the horizontal wind increases.

It is interesting to note that in period 1, the positive $u\eta$ peak is associated with a negative uw extrema. However, in periods 5 and 6, a negative $u\eta$ peak at the frequency of the wave spectrum peak is associated with a positive uw peak.

4.3 PHASE-COHERENCE RELATIONSHIPS

Phase and coherence relationships between the fluctuating wind components and the waves for periods 1-6 appear in Figures 13-18. In each figure, panels A-C and D-F are the u , v , and w spectra for the phase and coherence respectively.

The u -wave phase relationship in periods 3-6 is observed to be 160-180 degrees over a wide spectral band centered at the frequency of the wave spectra peaks (0.1 hz). Also, a high coherence value occurs at this frequency. This is indicative of high correlations between the fluctuating u

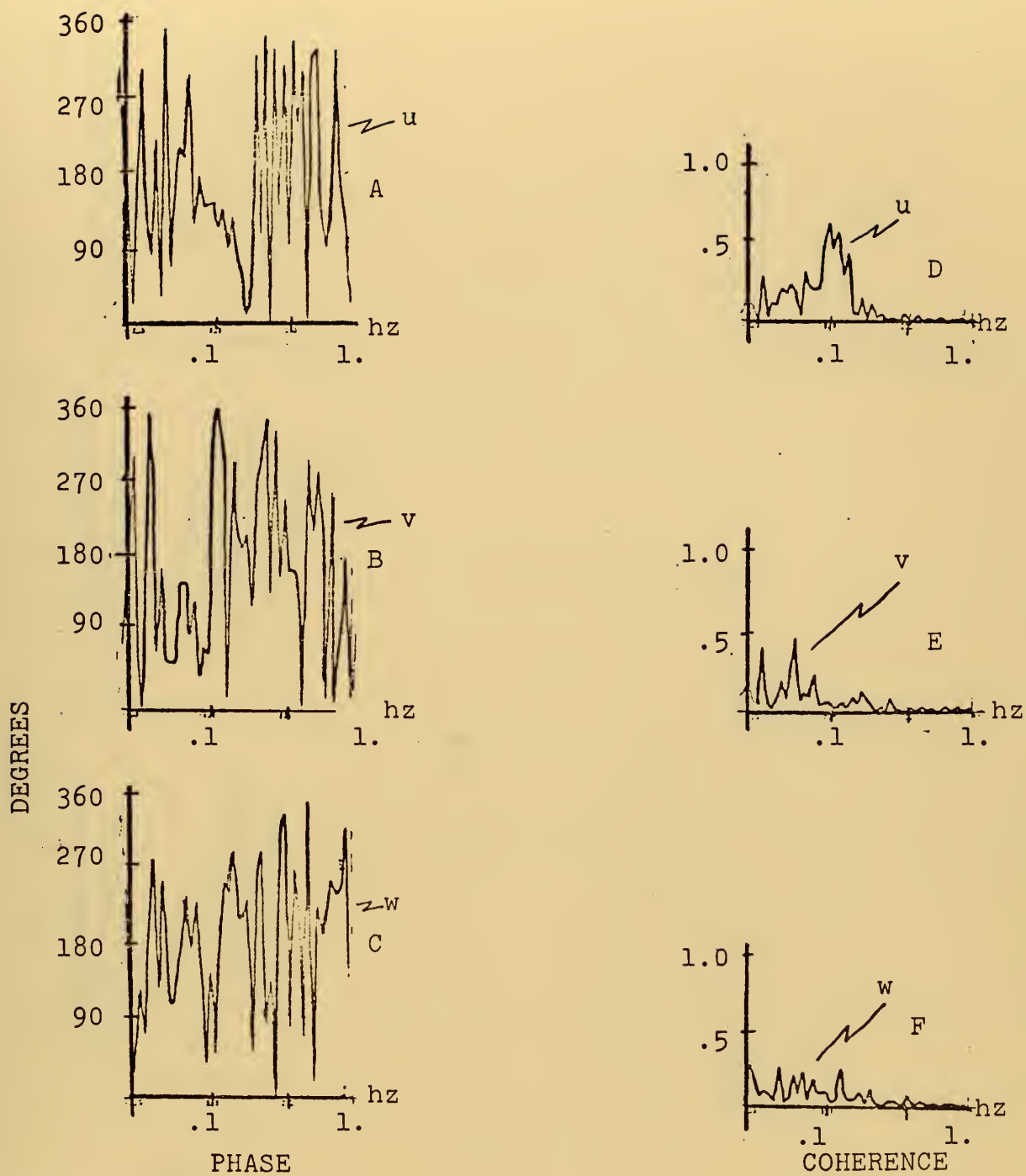


Figure 13. Period 1. Phase and Coherence Spectral Results

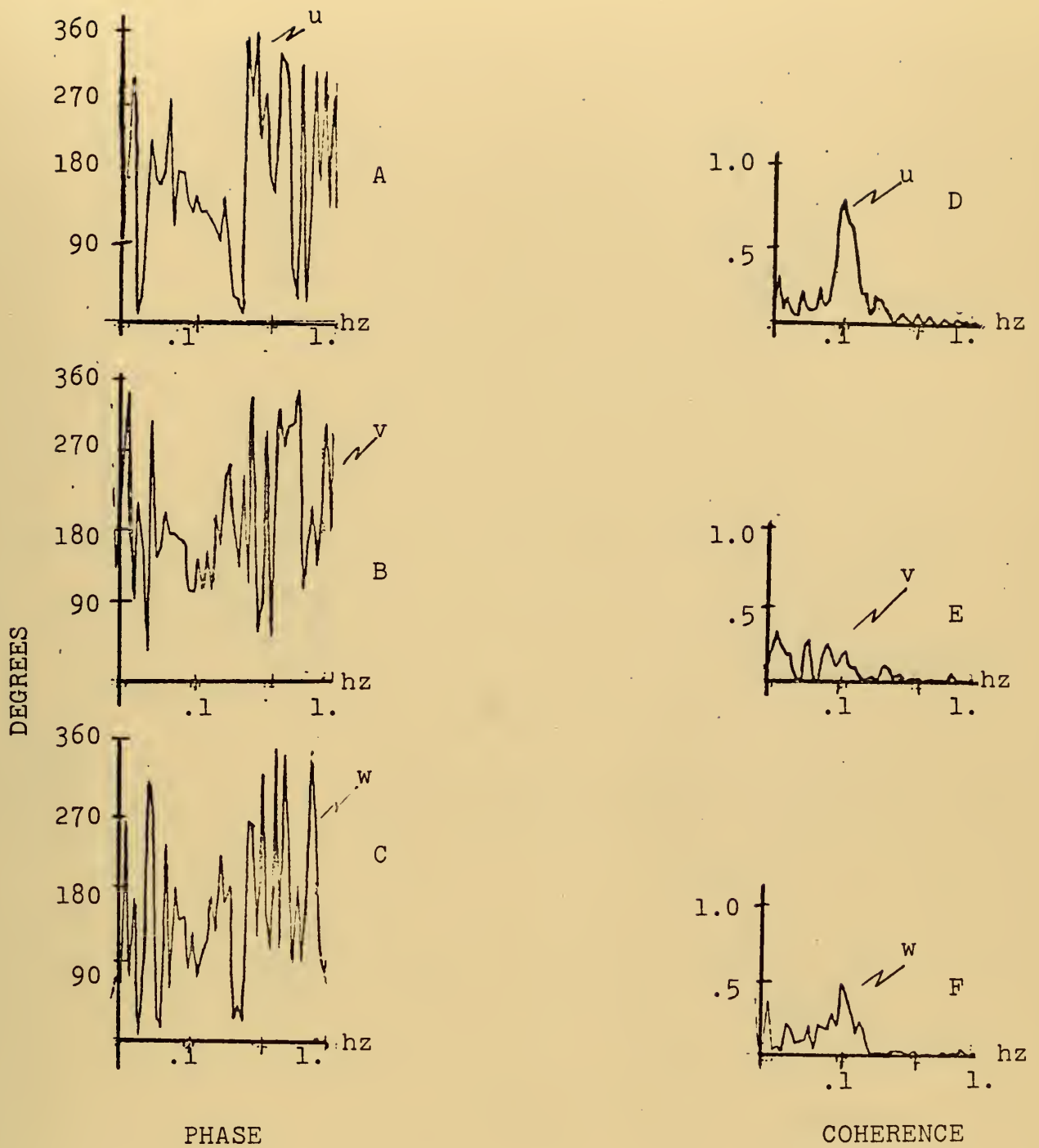
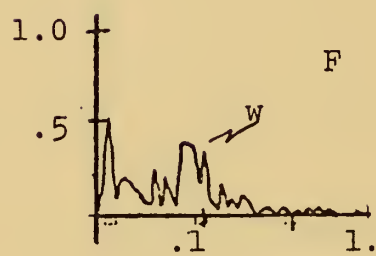
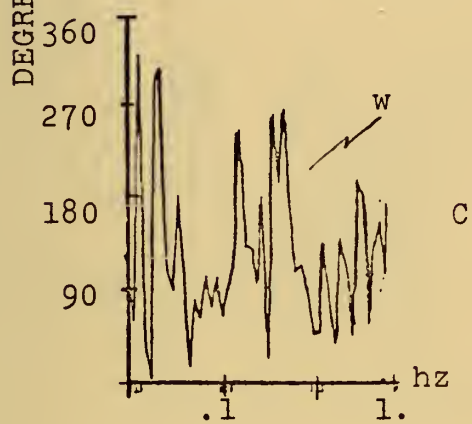
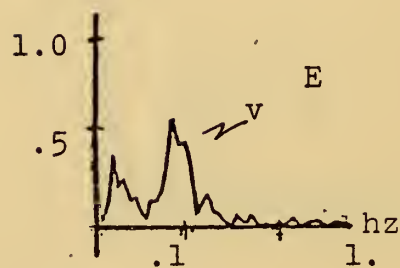
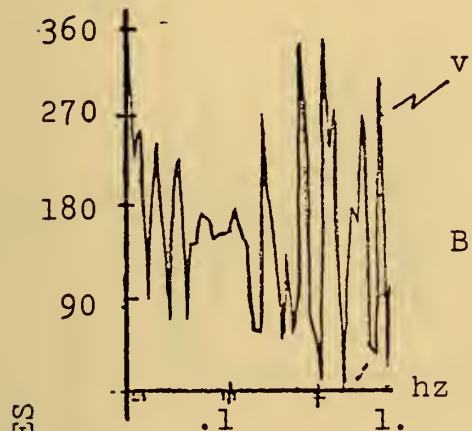
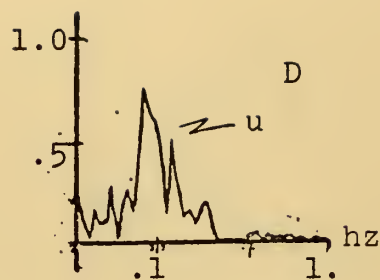
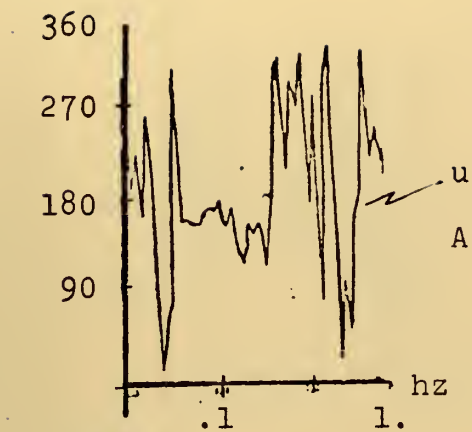


Figure 14. Period 2. Phase and Coherence Spectral Results



PHASE

COHERENCE

Figure 15. Period 3. Phase and Coherence Spectral Results

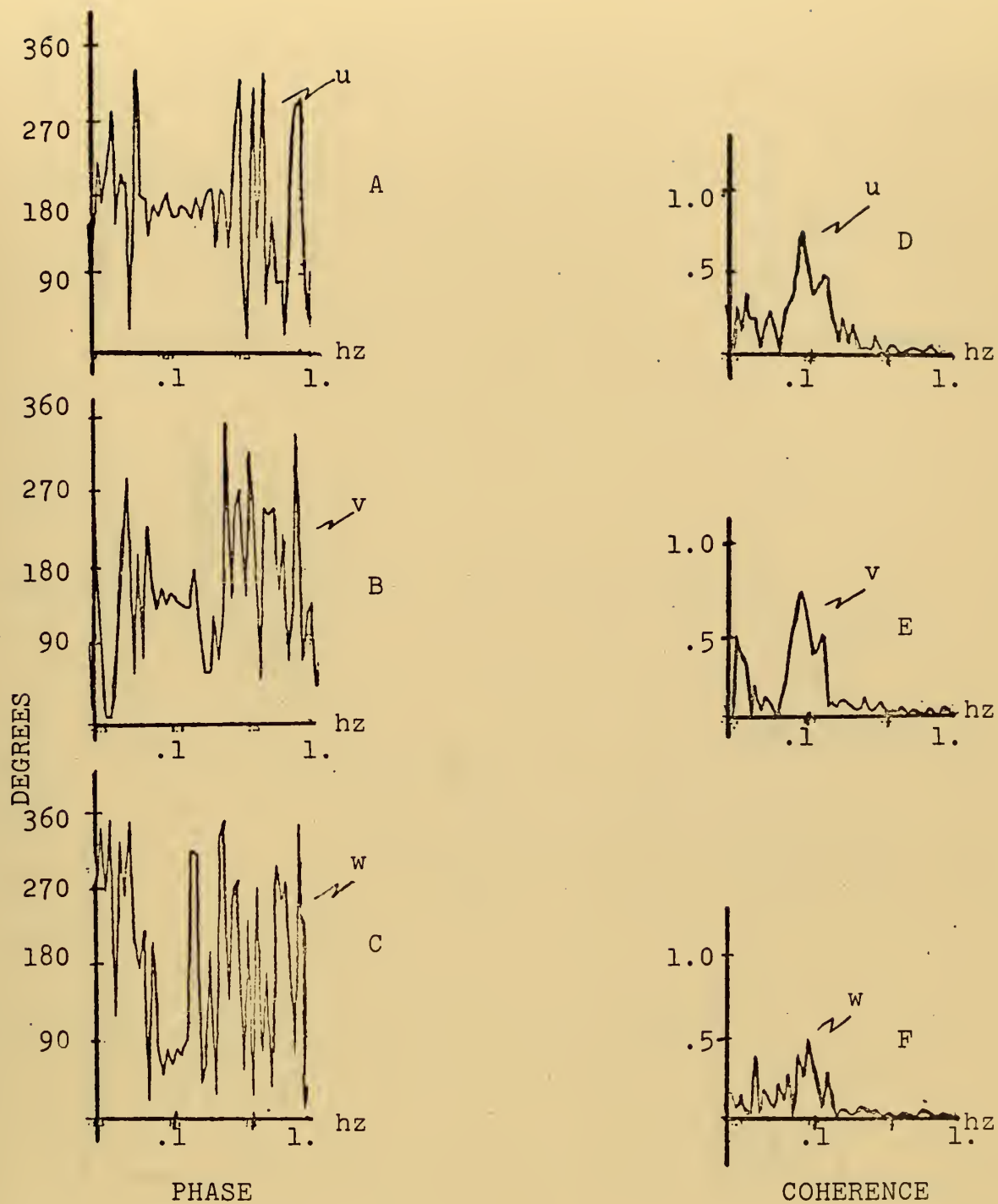


Figure 16. Period 4. Phase and Coherence Spectral Results

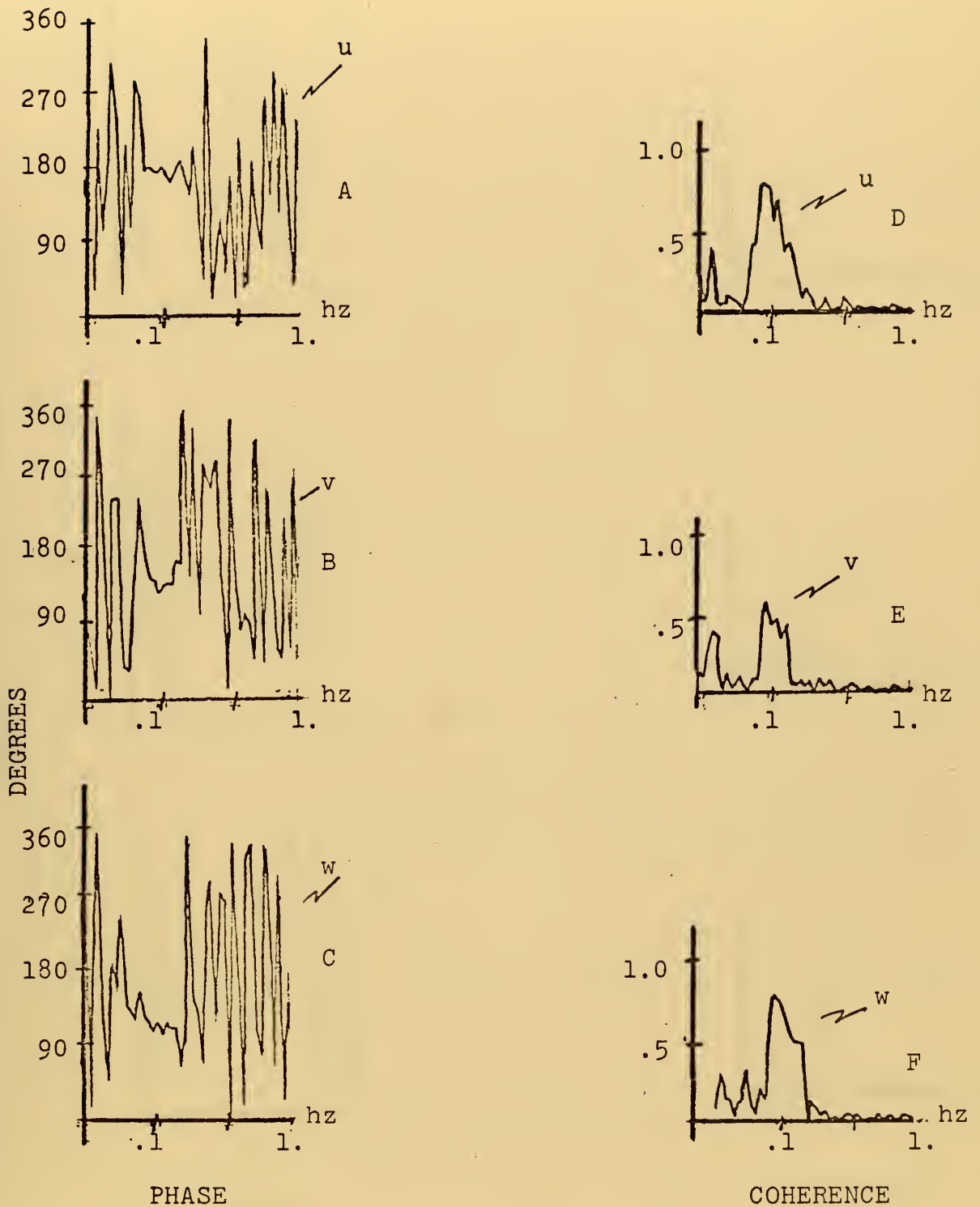


Figure 17. Period 5. Phase and Coherence Spectral Results

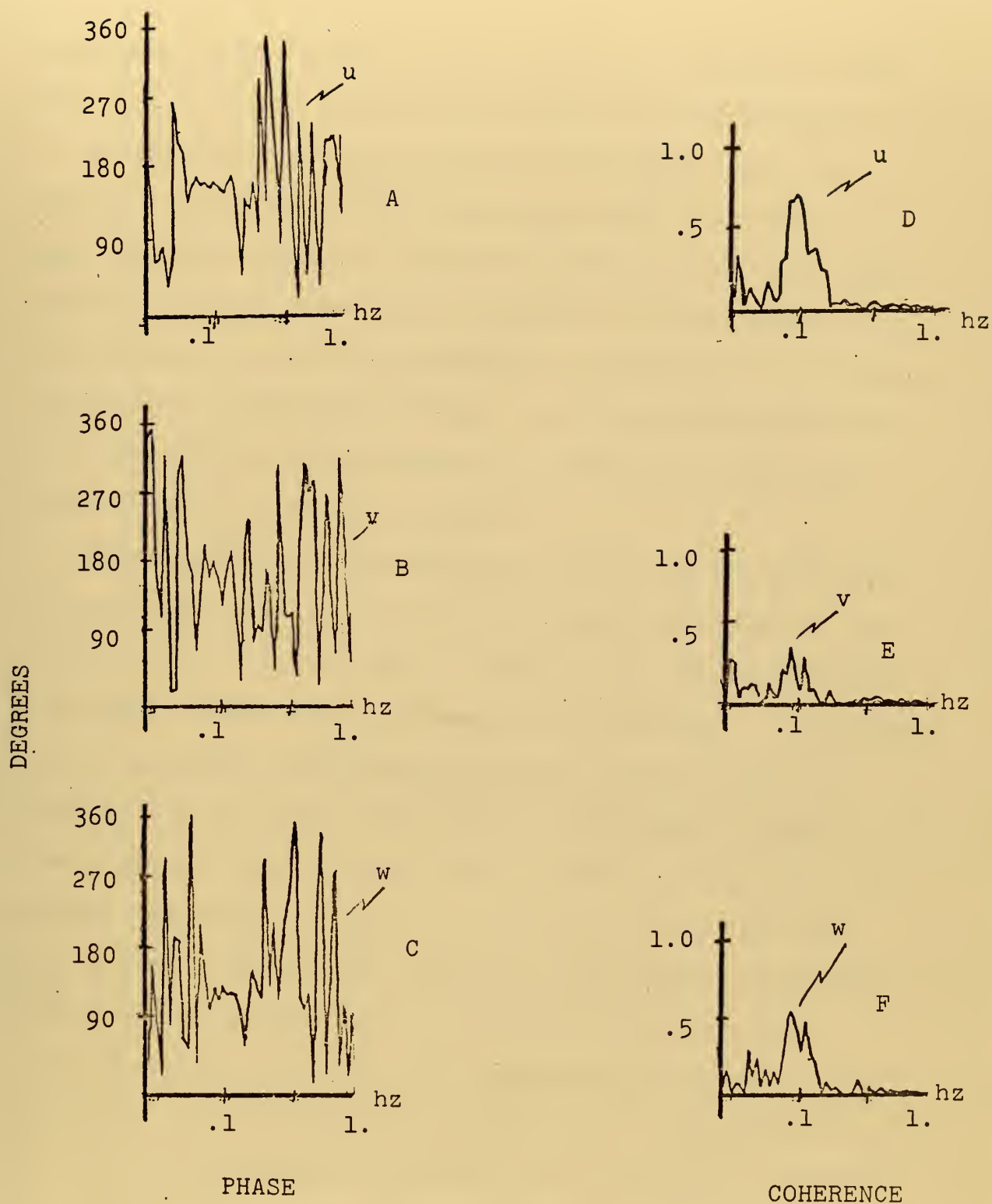


Figure 18. Period 6. Phase and Coherence Spectral Results

component and the waves. For u and w , the coherence value exceeds 0.5 at the frequency of the wave spectra peak.

In periods 1 and 2 the phase difference, about 180 degrees, at 0.1 hz steadily decreases with increasing frequency in the region of the wave spectra peaks. This phenomenon is perhaps due to the decrease of phase speed as the frequency of the wave component increases. Furthermore, significant correlation between u and the wave across this frequency band is substantiated by relatively high coherence values in these two periods.

Phase relationships between the lateral wind component and the waves are seen to obey the same predictions of potential flow that hold for u . For example, in periods 2-5, v depicts a phase difference of 160-180 degrees. In periods 1 and 6 no phase relationship between v and the waves is observed. Most likely, the periods depicting a v -wave phase relationship include a significant wave induced lateral wind component. Periods 2-5 also indicate relatively high values of coherence. This is, of course, a confidence factor in the interpretation of phase relationships.

Consideration of the w -wave phase relationships reveals a consistent correlation in periods 1-6. Interpretations of the relationships are supported by peak coherence values at the frequency of the wave spectra peaks. Again, as for u and v , the w -wave phase relationships approximate potential flow theory which predicts that w will lead the wave by 90 degrees. In period 1 background turbulence obscures the

phase relationship except over a very narrow spectral band centered at 0.1 hz. The corresponding coherence value is also observed to be very low. Periods 2-6 exhibit higher values of coherence (.4-.6) and the phase relations appear to exist over wider spectral bands.

The above described phase relationships were occurring at frequencies for which the phase speed exceeded the wind speed at the level of measurement. Therefore, these phase relationships represent conditions below the critical level and deviations from potential flow would be due to non-linear interactions resulting from turbulence in the airflow.

Very little evidence of linear wind-wave coupling has been observed. This is due to the fact that the critical level corresponding to the wave spectra peaks was well above 10 meters. However, any level of measurement in the near surface layer over a wave field with a continuous spectrum should be a critical level for some particular wave component.

On the basis of wind-wave coupling theories, it is recalled that at the critical level no phase relationships between the horizontal or vertical wind and the waves exist. On this respect, Kondo et al. noted that at some wave frequency whose phase speed was about $2/3$ the mean wind speed the phase relationship between u and the wave reversed abruptly and the coherence dropped to zero.

Considering the u -wave phase relationship again, an abrupt phase reversal occurs in all periods (1-6) at a

frequency of about 0.26 hz. The phase reversal is accompanied by a rapid approach of coherence toward zero at that same frequency.

To verify the phase reversal frequency appearing in the above results, an analysis technique of Kondo et al. was utilized. This technique incorporated use of the phase amplitude ratio. Recall the amplitude ratio is the ratio of the wave induced disturbance to the sea-surface displacement. Results obtained with the amplitude ratio technique are presented below.

4.4 AMPLITUDE RATIO RESULTS

Amplitude ratio results appear in Figures 19-21 where the values are plotted in a log-log format, with the y-axis scaled 0 to 1. A solid line denotes the smoothed curve.

The frequency at which the ratio of the wave induced disturbance to the sea surface displacement is a minimum, is near 0.26 hz. This wave component has a phase speed which is about equal to the mean wind speed at the level of measurement. Thus, the level of measurement is a critical level for the wave component at the frequency of the minima. In theory, the ratio would go to zero at the critical level because there is no wave induced motion at that level. However, the amplitude ratio minimum in these results does not actually approach zero due to the lack of a well defined critical level boundary and due to energy leakage from neighboring frequencies.

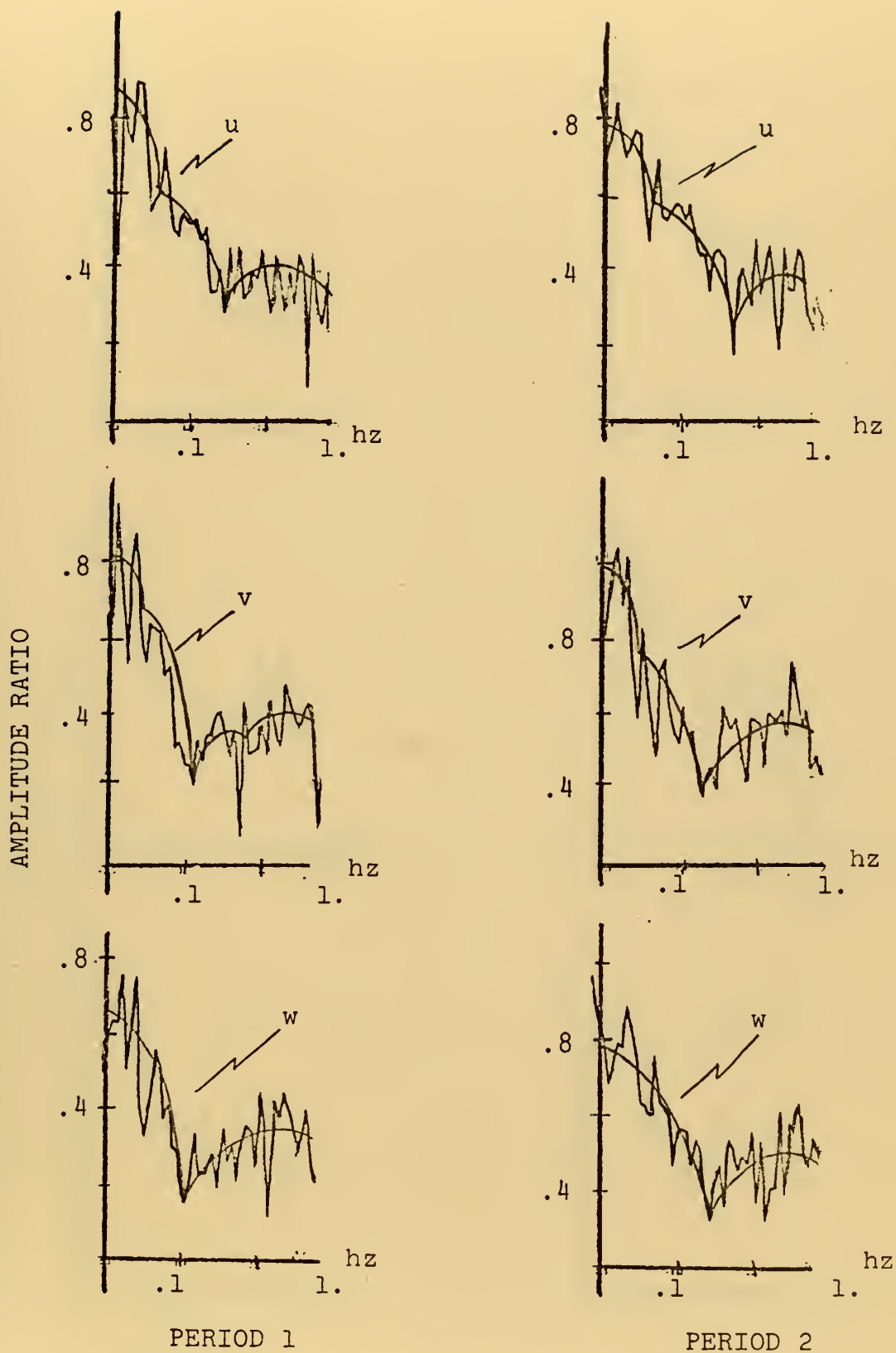


Figure 19. Amplitude Ratio Results

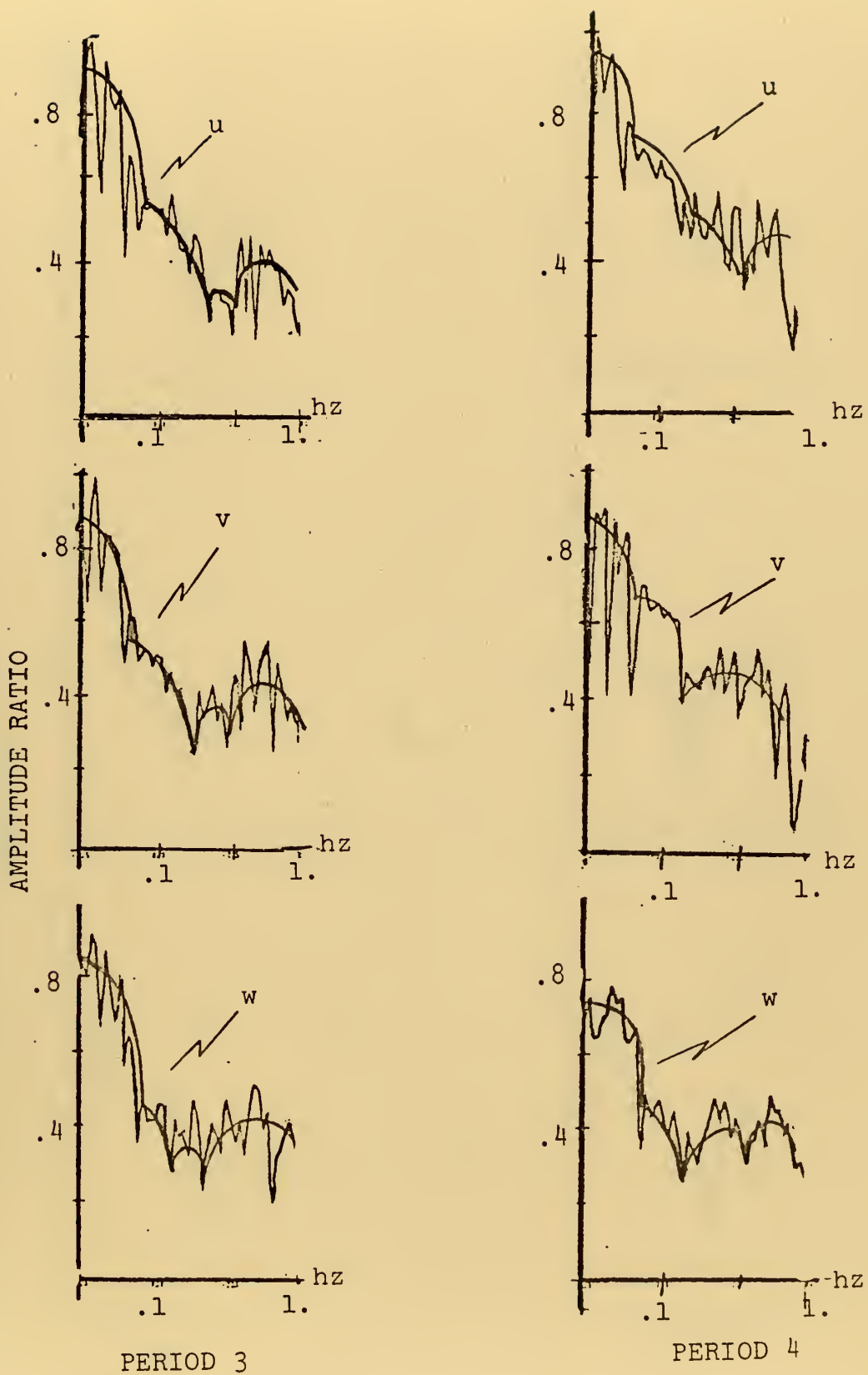


Figure 20. Amplitude Ratio Results

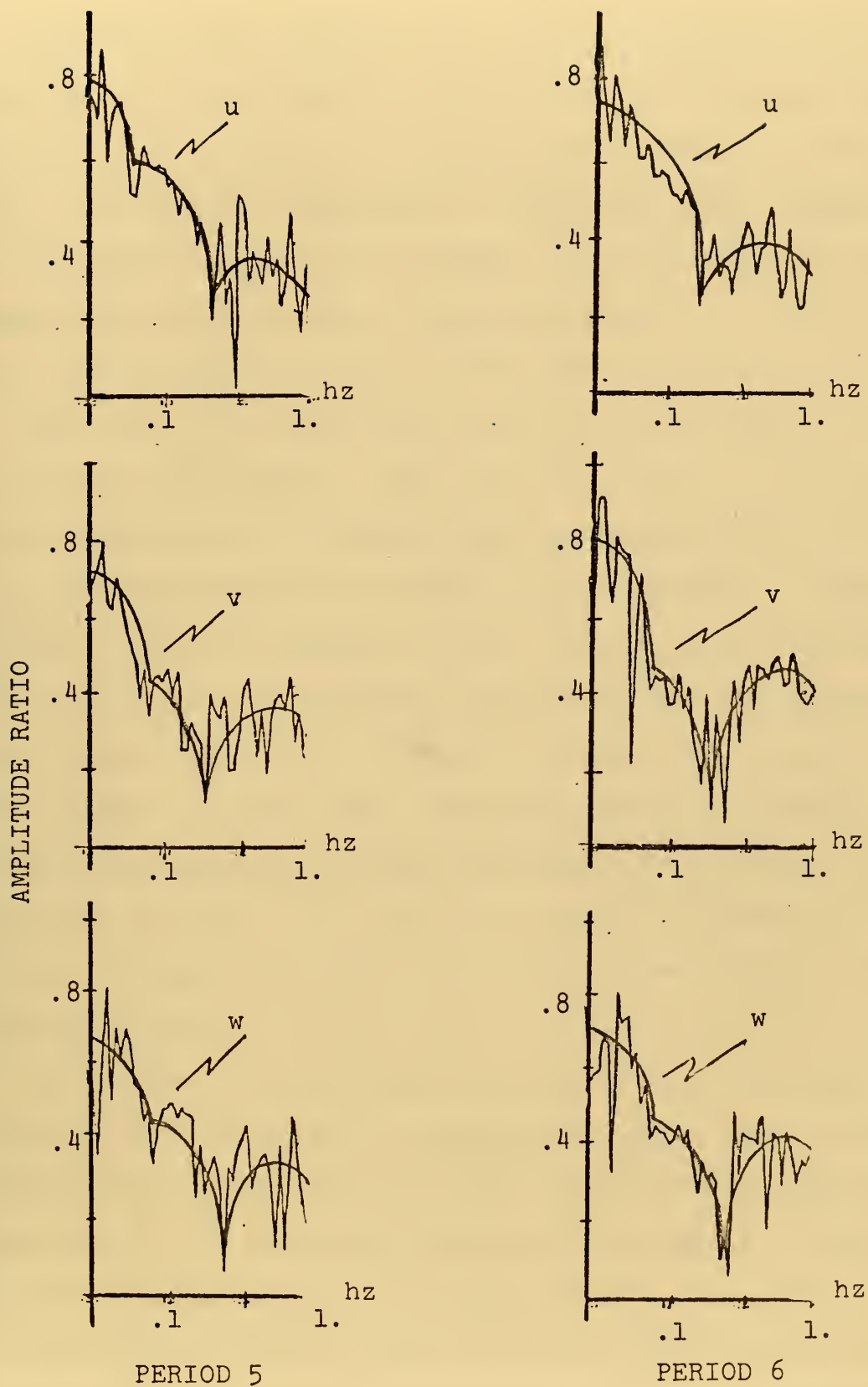


Figure 21.

Amplitude Ratio Results

Amplitude ratio minimums for v are also observed for each period, even though in two periods (1 and 6) the minimums are less distinct. It is significant that even for small lateral wind components an amplitude ratio minimum can be observed to exist. In contrast, the small lateral wind components gave only obscure spectral results in terms of power density peaks, phase, or coherence.

The ratio for w which was not considered by Kondo et al. will now be considered. Again, as for u and v , a distinct ratio minimum for w is observed at a frequency near 0.26 hz. This frequency also corresponds to the frequency of phase reversal and zero coherence for w . Recall that, in period 1 the w -wave phase relationship was obscure and the corresponding coherence value was low due to excessive background turbulence. However, the w ratio for period 1, clearly reveals the frequency at which the phase reversal and zero coherence occurred. In effect, the ratio minimum denotes the wave frequency for which the level of measurement was a critical level.

On the basis of the preceding discussion with regard to critical level features at frequencies higher than the predominate wave frequency, it is well to reexamine momentum transfer. It is noted that previous discussions on the co-spectra emphasized the non-linear transfer since the critical level corresponding to the wave spectrum peak was effectively at infinity. Examination of the uw co-spectra in period 5 and 6 (Figures 11 and 12) reveals that enhanced

downward momentum transfer occurs on the high frequency side of the wave spectra peaks. These observations agree with the predictions from Miles' theory which states that at the critical level momentum is taken from the airflow and transferred downward, resulting in exponential wave growth.

4.5 RESULTS AT THE 3 METER LEVEL (PERIOD 7)

Period 7 results (Figures 22-24) represent measurements at the 3 meter level as compared to the 8 meter level measurement in the other 6 periods.

As for the higher levels, pronounced peaks in the u , v , w spectra correspond to the frequency of the wave spectrum peak (near 0.1 hz). Interestingly, a negative uw momentum transport is observed even though the level of measurement is well below the critical level. Also observed is positive un co-spectra at 0.1 hz. In Figure 23, the phase reversal of u and v occur at the same frequency as the minimum amplitude ratio in Figure 24. This frequency is higher than found in the other periods because the mean wind speed at this level is less. This agrees with Kondo who found the ratio minimum to be dependent on height and mean wind velocity at that level. The w phase shift of 330 degrees will go unexplained. However, the ratio and coherence for w are consistent.

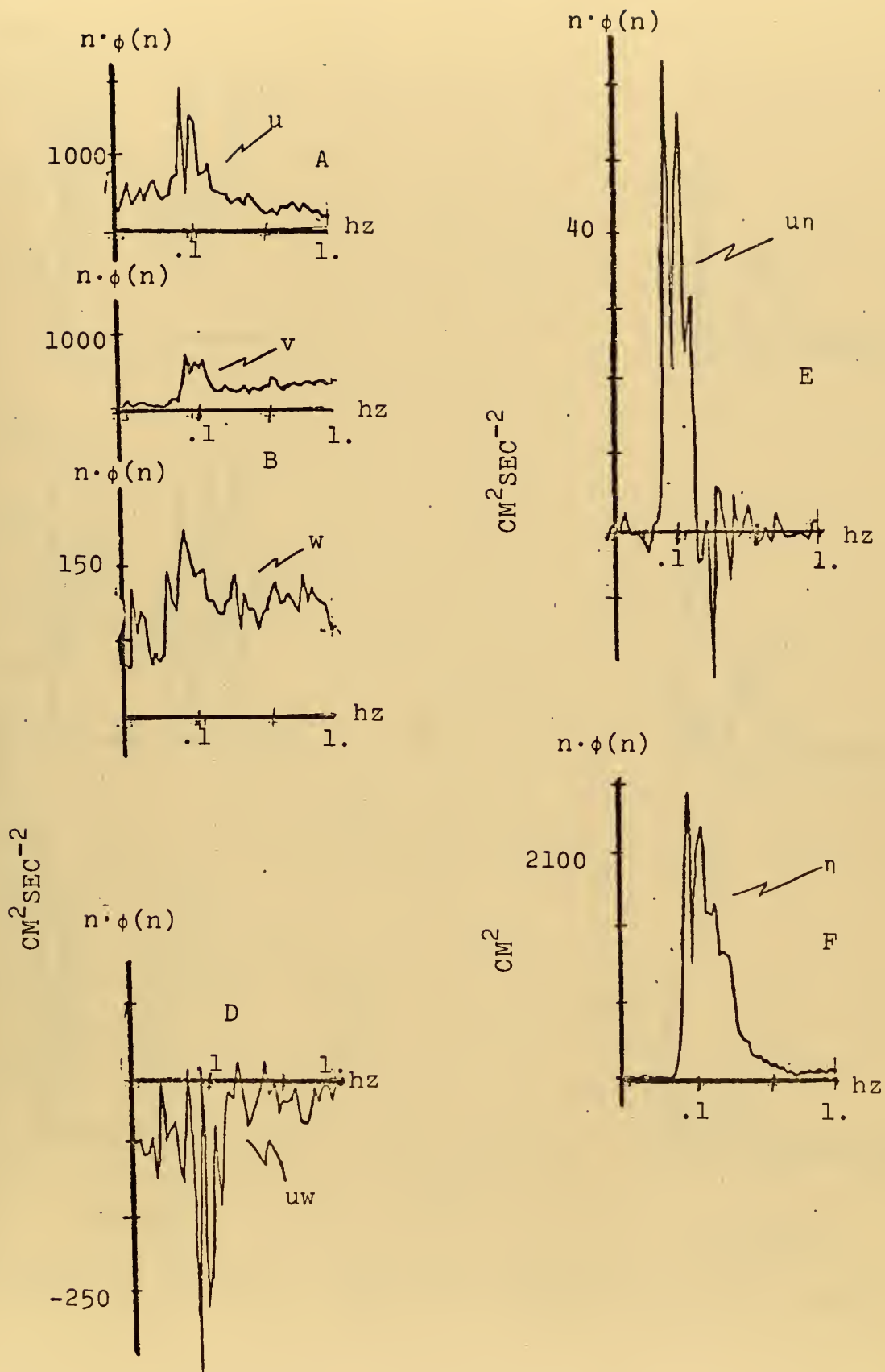
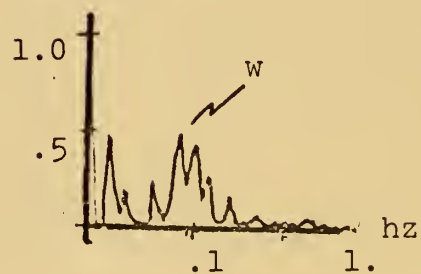
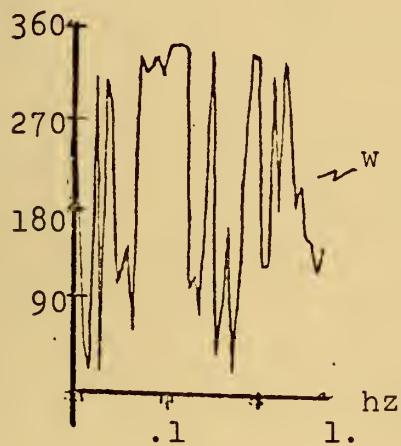
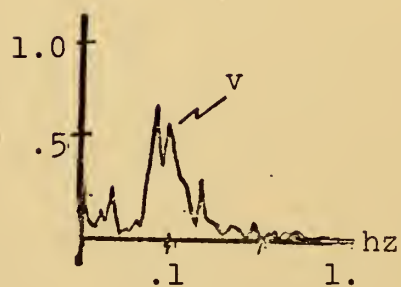
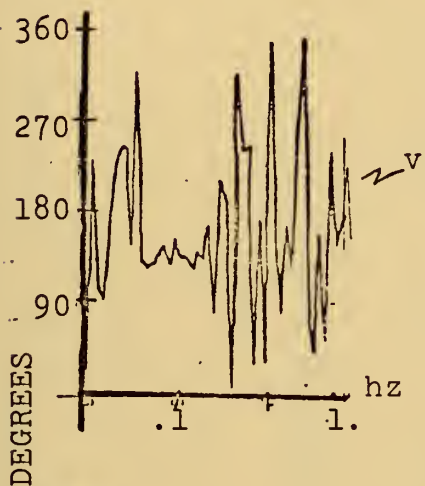
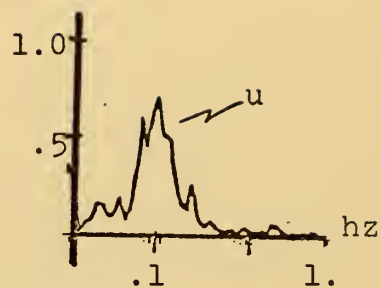
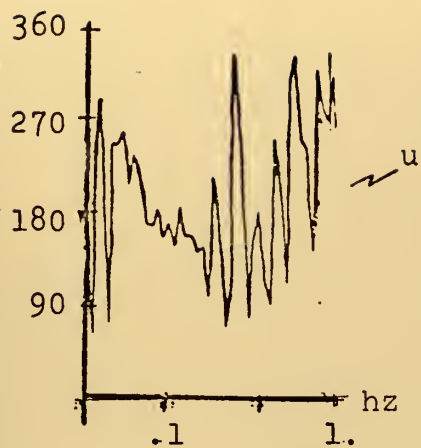


Figure 22. Period 7. Variance and Covariance Spectral Results



PHASE

COHERENCE

Figure 23. Period 7. Phase and Coherence Spectral Results

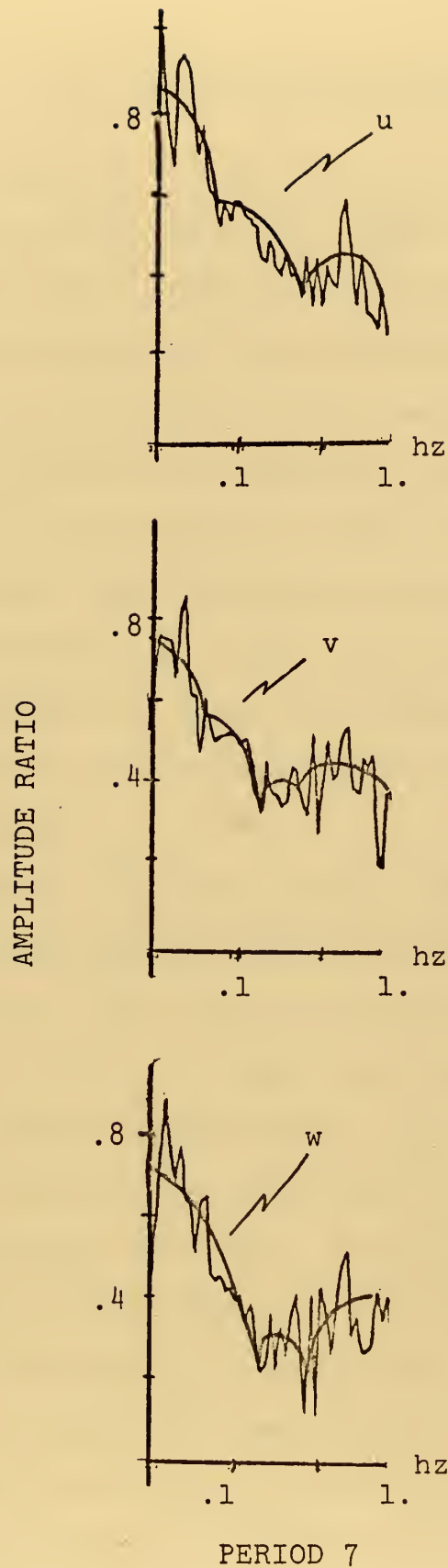


Figure 24. Amplitude Ratio Results

V. SUMMARY AND CONCLUSIONS

Spectral analyses were performed on turbulence data obtained over ocean waves during BOMEX. Results of seven selected periods were examined with respect to predictions in recent non-linear and linear wind-wave coupling theories.

Initial interpretation of the spectral results pertained to non-linear interaction between the wave-induced motion and turbulence in the airflow. Peaks in the velocity spectra occurred at the frequency of the wave spectra peaks. At this same frequency (0.1 hz) upward transfer of u momentum, uw , was observed. Phase relationships were in partial agreement with the predictions of potential flow theory in the spectral region.

At a frequency (0.26 hz) slightly higher than that of the wave spectrum peak the wind-wave phase relationship changes abruptly. This change occurred at a frequency where the wave phase speed was roughly two-thirds the mean wind speed at the level of measurement. At this same frequency the wind-wave correlation approached zero, and increased momentum transfer was observed. An examination of the amplitude ratio results confirmed the frequency of minimum wave induced disturbance to be at about 0.26 hz.

Basic conclusions from these results are:

1. The spectral results of this study are in general agreement with the results of Kondo et al. and Davidson, and provide more evidence that wind-wave

coupling is significant and occurs, perhaps, as predicted by the models of Miles and Yefimov.

2. The results indicate that simultaneous investigation of both linear and non-linear aspects of wind-wave coupling are feasible in observational studies independent of wind and wave conditions. This is because every level of measurement is a critical level for some component of the wave spectrum and both linear and non-linear processes are occurring simultaneously.

BIBLIOGRAPHY

1. Bronson, E.D., and Glasten, L.R., FLIP, FLOATING INSTRUMENT PLATFORM, SIO Reference 65-12, ONR Contract Nonr 2216 (05), Scripps Institute of Oceanography, San Diego, Cal. 21 pp.
2. Cooley, J.W. and Tukey, J.W., "Algorithm for the Machine Calculations of Complex Fourier Series," Math of Comp., 19(90), p. 297-301, 1965.
3. Davidson, K.L., An Investigation of the Influence of Water Waves on the Adjacent Airflow, ORA Report 08849-2-T, ONR Contract N00014-67-A-0181-0005, Dept. of Meteor. and Ocean., University of Michigan, 259 pp, 1970.
4. Davidson, K.L., and Frank, A.J., "Properties of Wave-related Fluctuations in the Airflow above Natural Waves," J. Phy. Ocean., 3(1), (In press, will appear in Jan 73).
5. Harris, D.L., "The Wave Driven Wind", J. Atmos. Sci., 23(6), pp. 688-698, 1962.
6. Jeffreys, H., "On the Formation of Waves by Wind", Proc. Royal Soc., A 107, pp. 189-206, 1924.
7. Kondo, J., Fujinawa, Y., and Naito, G., "Wave-Induced Wind Fluctuation over the sea", J. Fluid Mech. Vol. 51. Part 4, pp. 751-771, 1972.
8. Lighthill, M.J., "Physical Interpretation of the Mathematical Theory of Wave Generation by Wind," J. Fluid Mech., 14(3), pp. 385-398, 1962.
9. Lumley, J.L. and Panofsky, H.A., The Structure of Atmospheric Turbulence, John Wiley and Sons, Inc., New York, 231 pp., 1964.
10. Miles, J.W., "On the Generation of Surface Waves by Shear Flows," J. Fluid Mech., 3(2), pp. 185-204, 1957.
11. Miles, J.W., "On the Generation of Surface Waves by Shear Flows," J. Fluid Mech., 6(4), pp. 568-582, 1959.
12. Miles, J.W., "A Note on the Interaction between Surface Waves and Wind Profiles," J. Fluid Mech., 22(4), p. 823-827, 1965.

13. Miles, J.W., "On the Generation of Surface Waves by Turbulent Shear Flows," J. Fluid Mech., 7(3), p. 469-478, 1960.
14. Cort, A.H. and Taylor, A., "On the Kinetic Energy Spectrum near the Ground," Mon. Wea. Review, 97(9), p. 623-636, 1969.
15. Phillips, O.M., "On the Generation of Waves by Turbulent Wind," J. Fluid Mech., 2(5), p. 417-445, 1957.
16. Pond, S., Phelps, G.T. and Paquin, J.E., "Measurements of the Turbulent Fluxes of Momentum, Moisture and Sensible Heat over the Ocean," J. Atmos. Sci., Vol. 28, No. 6, Sept. 1971.
17. Portman, D.T., Davidson, K.L., Walter, M.A., An Investigation Of the Structure of Turbulence and of the Turbulent Fluxes Of Momentum and Heat over Waves, ORA Report 08849-3-P, ONR Contract N0014,67-A-0181-0005, Dept. of Meteor. and Ocean., U. of Michigan, 40 pp., 1970.
18. Stewart, R.W., "Mechanics of the Air-Sea Interface," Physics of Fluids Supplement, 10, S189-S194, 1967.
19. Superior, W.J., BOMEX Flux and Profile Measurements from FLIP. Final Report, Naval Oceanographic Office Contract N62306-69-C-0186, C.W. Thornthwaite Associates, Laboratory of Climatology, Elmer, N.J., 32 pp., 1969.
20. Yefimov, V.V., "On the Structure of the Wind Velocity Field in the Atmospheric Near-Water Layer and Transfer of Wind Energy to Sea Waves.", IZV, Atmospheric and Oceanic Physics, Academy of Sciences, USSR, 5 Eng. Trans. A. Peiperl, p. 530-537, 1969.
21. Yefimov, V.V. and Sizov, A.A., "Experimental Study of the Field of Wind Velocity over Waves." IZV, Atmospheric and Oceanic Physics, Academy of Sciences, USSR, 5, Eng. Trans. A. Peiperl, p. 530-537, 1969.
22. Zilitinkevich, S.S. "On the Calculation of Global Phenomena of the Interaction between the Oceans and the Atmosphere", IZV, Atmospheric and Oceanic Physics, Academy of Sciences, USSR, 5(11), Eng. Trans. A.B. Kaufman, p. 1143-1159, 1969.

INITIAL DISTRIBUTION LIST

	No. Copies
1. Defense Documentation Center Cameron Station Alexandria, Virginia 22314	2
2. Library, Code 0212 Naval Postgraduate School Monterey, California 93940	2
3. Professor Kenneth L. Davidson, Code 51Ds Department of Meteorology Naval Postgraduate School Monterey, California 93940	5
4. Lieutenant Commander Glenn S. Bingham USN RVAW 110 NAS North Island, California 92135	3
5. Professor Noel Boston, Code 58Bb Department of Oceanography Naval Postgraduate School Monterey, California 93940	1
6. Professor Edward Thornton, Code 58Tm Department of Oceanography Naval Postgraduate School Monterey, California 93940	1
7. Department of Meteorology Naval Postgraduate School Monterey, California 93940	2
8. Professor G. J. Haltiner, Code 51Ha Department of Meteorology Naval Postgraduate School Monterey, California 93940	1
9. Dr. Donald J. Portman Department of Meteorology and Oceanography University of Michigan Ann Arbor, Michigan 48103	1
10. Professor R. T. Williams, Code 51Wu Department of Meteorology Naval Postgraduate School Monterey, California 93940	1

11. Commander, Naval Weather Service Command 1
Naval Weather Service Headquarters
Washington Navy Yard
Washington, D. C. 20390
12. Professor Arthur L. Schoenstadt, Code 53Zh 1
Department of Mathematics
Naval Postgraduate School
Monterey, California 93940
13. Lieutenant David M. Ihle, USN 1
USS CALOOSAHATCHEE (AO 98)
FPO, New York 09501

DOCUMENT CONTROL DATA - R & D

(Security classification of title, body of abstract and indexing annotation must be entered when the overall report is classified)

1. ORIGINATING ACTIVITY (Corporate author) Naval Postgraduate School Monterey, California 93940		2a. REPORT SECURITY CLASSIFICATION Unclassified	
		2b. GROUP	
3. REPORT TITLE Spectra of Turbulent Fluctuations over Ocean Waves			
4. DESCRIPTIVE NOTES (Type of report and inclusive dates) Master's Thesis; September 1972			
5. AUTHOR(S) (First name, middle initial, last name) Glenn Stevenson Bingham			
6. REPORT DATE September 1972		7a. TOTAL NO. OF PAGES 64	7b. NO. OF REFS 22
6a. CONTRACT OR GRANT NO.		9a. ORIGINATOR'S REPORT NUMBER(S)	
b. PROJECT NO.			
c.		9b. OTHER REPORT NO(S) (Any other numbers that may be assigned this report)	
d.			
10. DISTRIBUTION STATEMENT Approved for public release; distribution unlimited.			
11. SUPPLEMENTARY NOTES		12. SPONSORING MILITARY ACTIVITY Naval Postgraduate School Monterey, California 93940	
13. ABSTRACT Spectral analyses are performed on turbulence data obtained over natural ocean waves during BOMEX. Results are obtained for variance and co-variance spectra, phase and coherence relationships, and amplitude ratios. Peaks in the horizontal and vertical velocity spectra are observed to correspond to the frequency of the wave spectra peaks. Phase relationships tend to obey predictions of potential flow theory in regions of the wave spectra peaks. However, the wave related motion contributes to the momentum transfer which is not predicted by potential flow theory. The ratio of the wave induced disturbance to the sea surface displacement is used to locate the wave spectra frequency for which the level of measurement is a critical level. Results of the study are readily compared to existing wind-wave coupling theories, both linear and non-linear.			

KEY WORDS

LINK A

LINK B

LINK C

ROLE

WT

ROLE

WT

ROLE

WT

Turbulence

Wave-induced motion

Observational data

Potential flow predictions

Wind-wave coupling

Spectral Analysis

BOMEX

Sea-Air Interaction

7 SEP 77

24920

Thesis

B5427

c.1

Bingham

138068

Spectra of turbulent
fluctuations over ocean
waves.

7 SEP 77

24920

Thesis

B5427

c.1

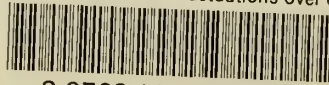
Bingham

138068

Spectra of turbulent
fluctuations over ocean
waves.

thesB5427

Spectra of turbulent fluctuations over o



3 2768 002 13465 2

DUDLEY KNOX LIBRARY